

Exploration with LHCb: from unseen to rare

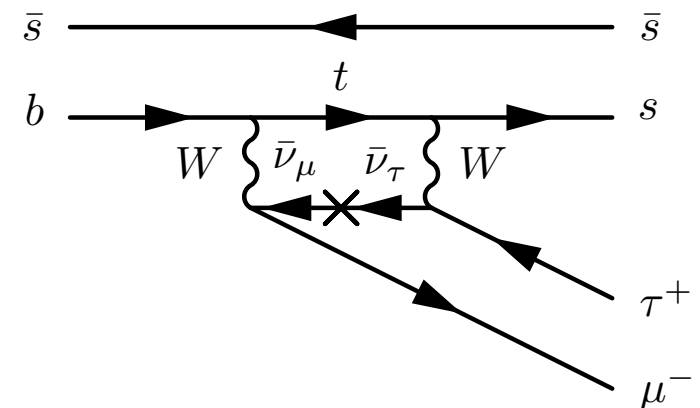
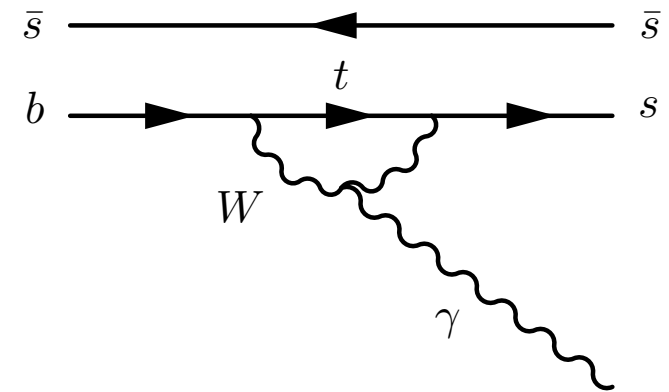
Lesya Shchutska

EPFL

on behalf of the LHCb Collaboration

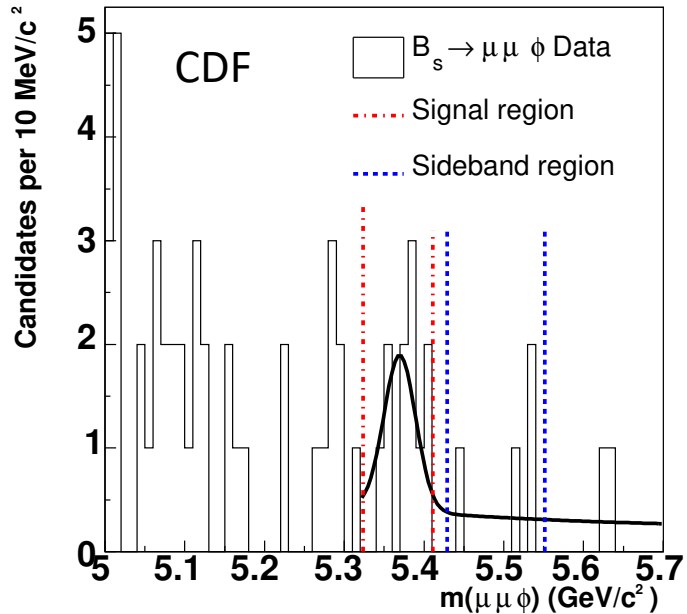
Rare decays – test-ground for unknown

- **Flavor-changing neutral current** processes $q \rightarrow q' \gamma$ and $q \rightarrow q' \ell^+ \ell^-$ are forbidden at the tree-level in the SM:
 - proceed at the loop level \Rightarrow suppressed in the SM
 - can be sensitive to virtual BSM particles in the loop
 - benefit from precise SM predictions
- **Decays forbidden in the SM** or beyond experimental reach $q \rightarrow q' \ell^+ \ell'^-$
 - observation will be a clear sign of BSM
- \Rightarrow **Rare decays allow for model-independent BSM searches**



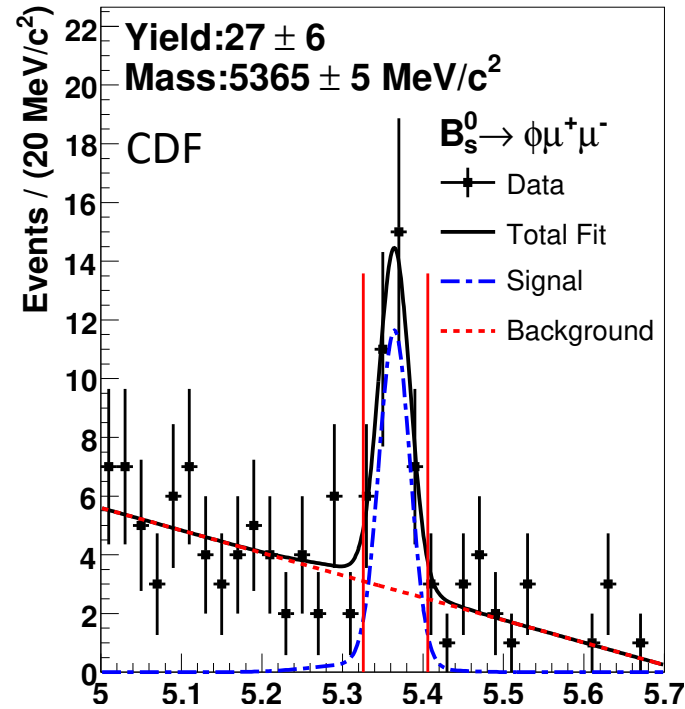
An exploration: $B_s^0 \rightarrow \phi\mu\mu$ from unseen to rare

Search for ...



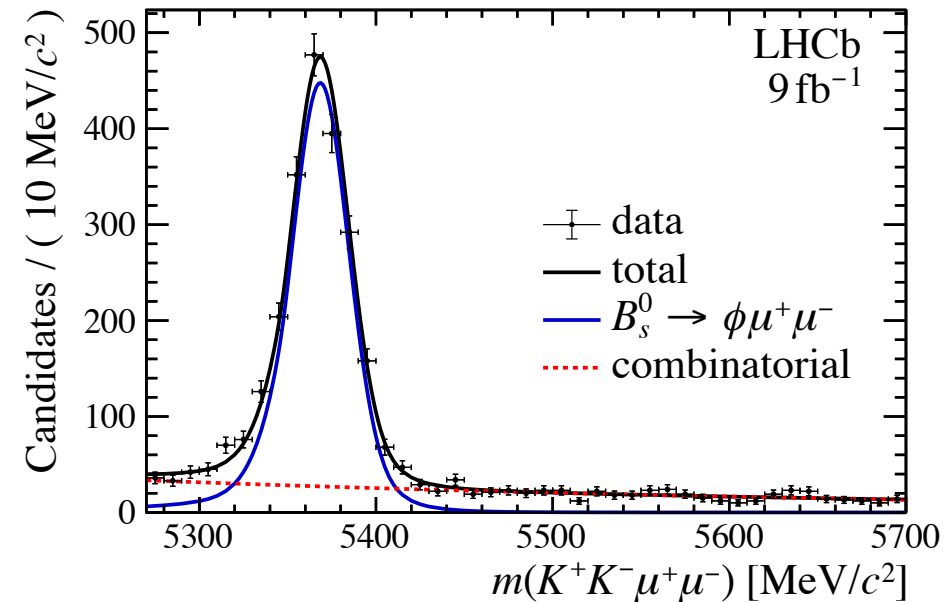
[Phys.Rev.D 79 \(2009\) 011104](#)

First observation of ...



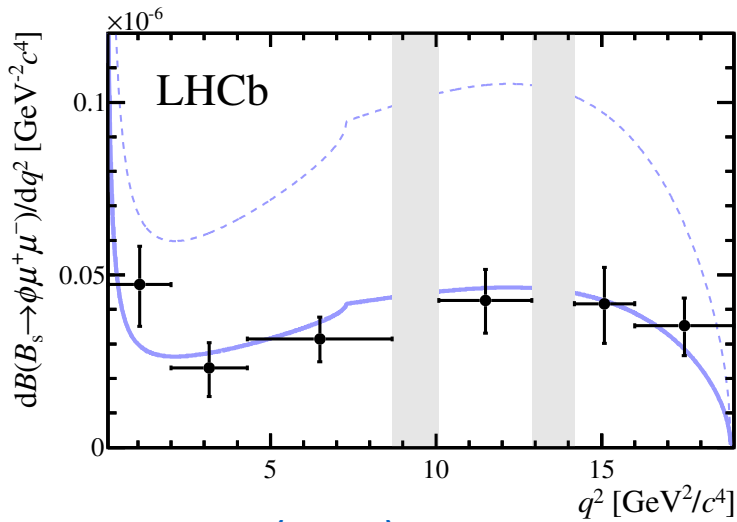
[Phys.Rev.Lett. 106 \(2011\) 161801](#)

Measurements of ...



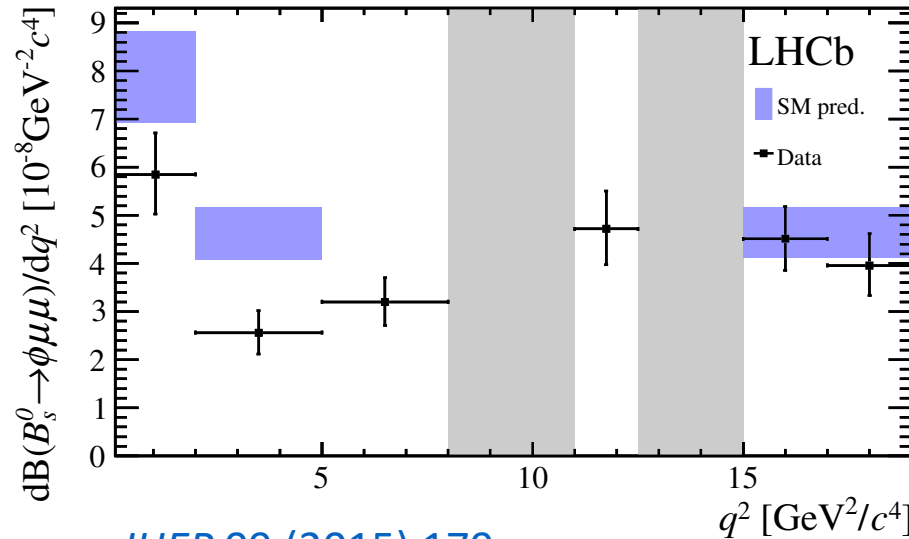
[Phys.Rev.Lett. 127 \(2021\) 151801](#)

.... to differential BFs and their puzzles

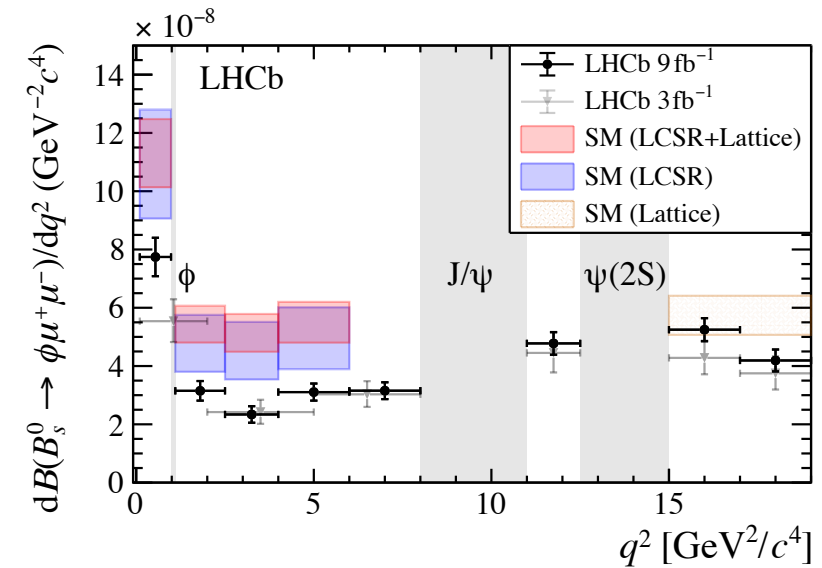


[JHEP 07 \(2013\) 084](#)

Differential branching fraction measurement and angular analysis of ...

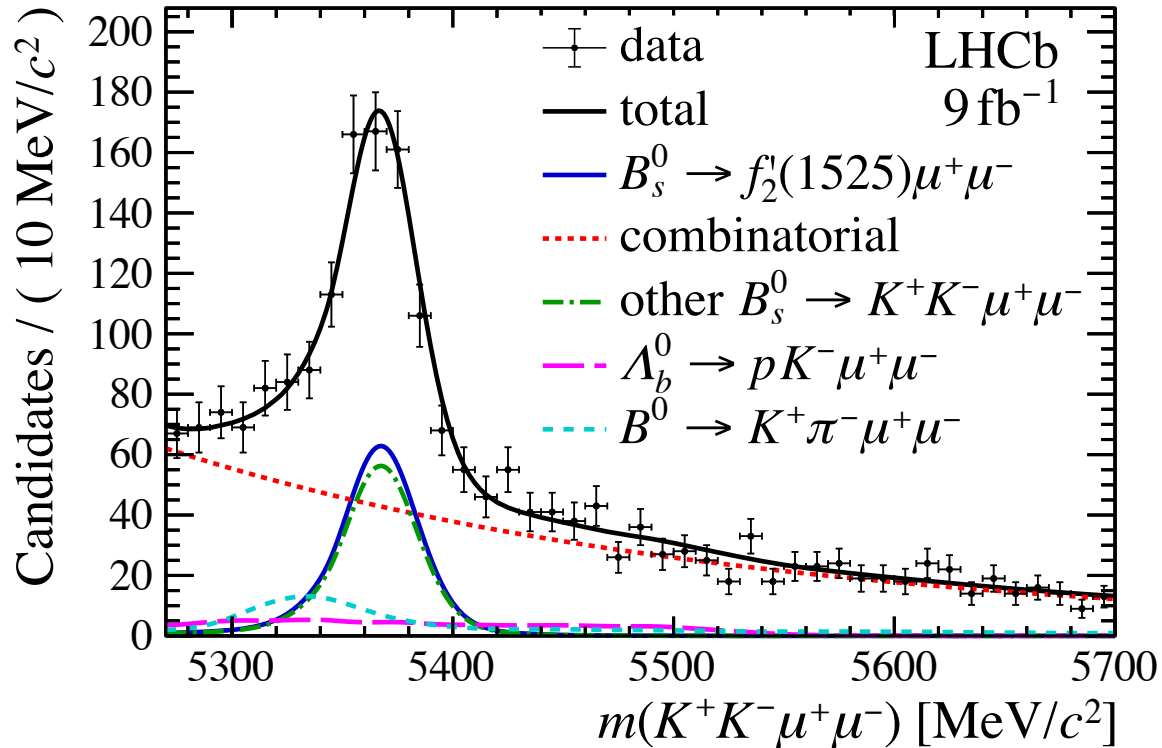


[JHEP 09 \(2015\) 179](#)

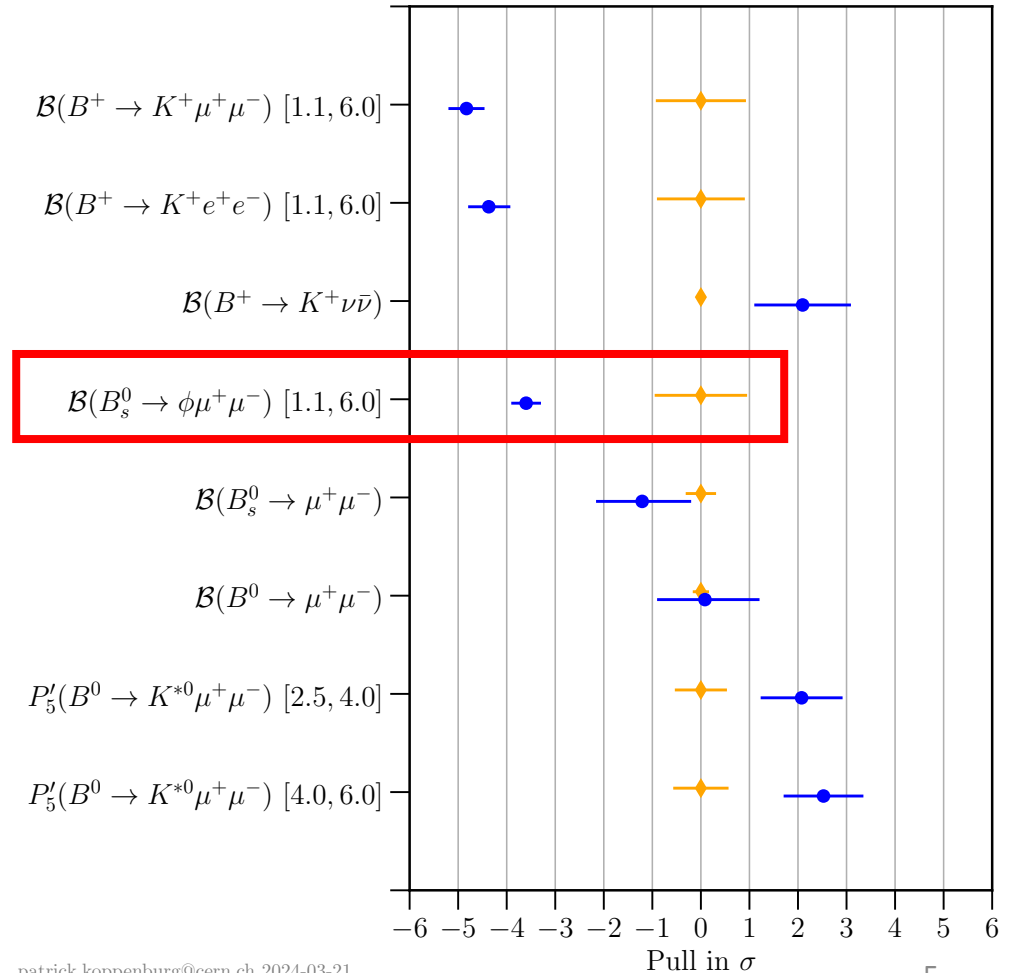


[Phys.Rev.Lett. 127 \(2021\) 151801](#)

A new chapter: $B_s^0 \rightarrow f_2'(1525)\mu\mu$



- $\mathcal{B}(B_s^0 \rightarrow f_2'(1525)\mu\mu)$ broadly agrees with the SM
- while $B_s^0 \rightarrow \phi\mu\mu$ is 3.6σ below the theory
- \Rightarrow collecting more data and exploring new channels!

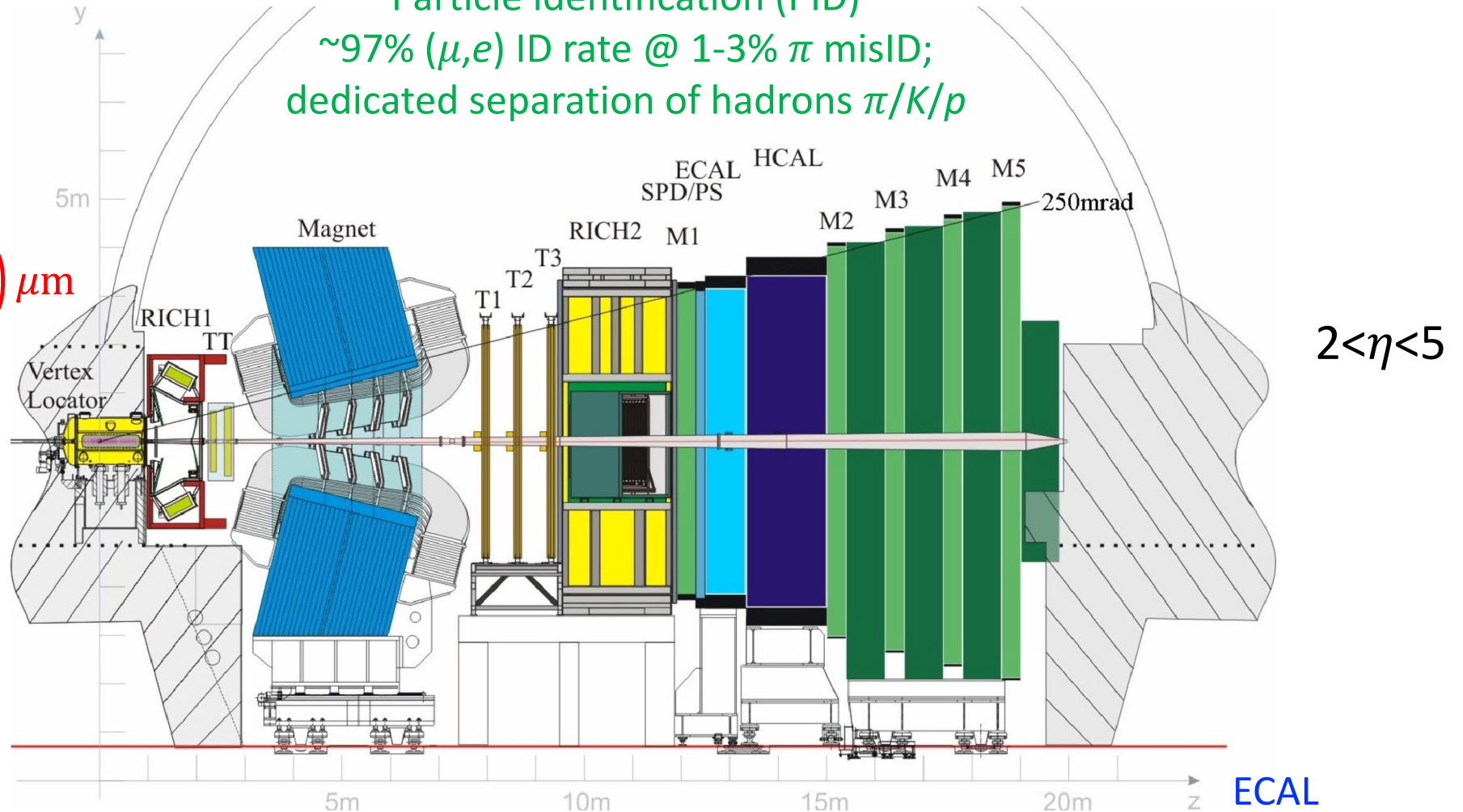


The LHCb detector

Particle identification (PID)
 ~97% (μ, e) ID rate @ 1-3% π misID;
 dedicated separation of hadrons $\pi/K/p$

$$\sigma_{IP} = \left(15 + \frac{29}{p_T(\text{GeV})} \right) \mu\text{m}$$

VELO



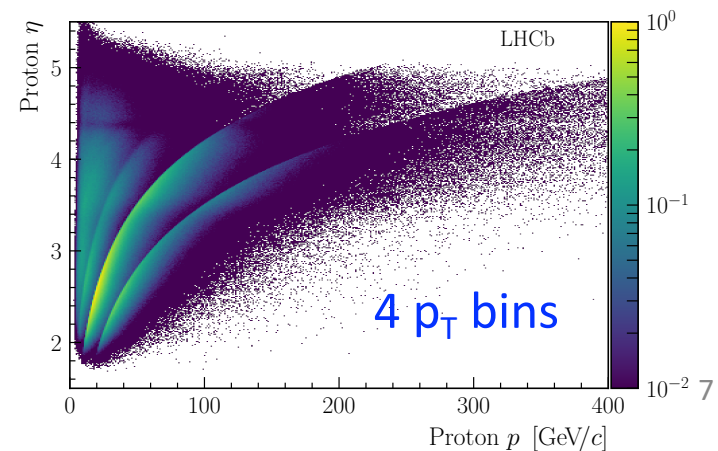
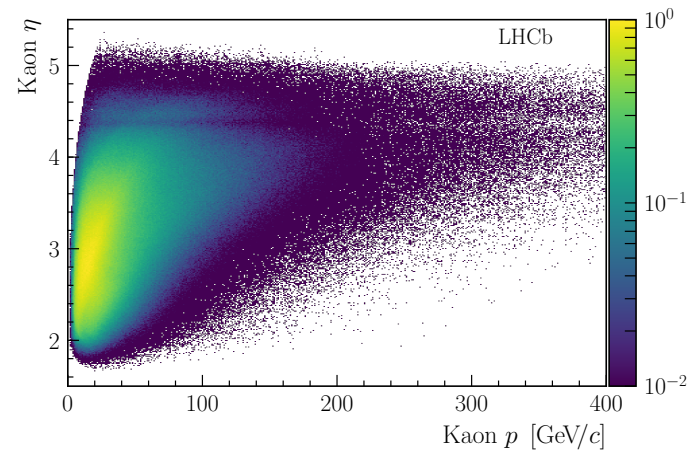
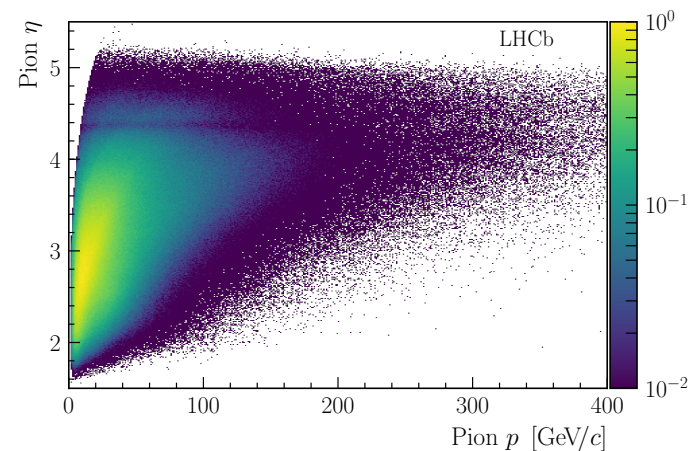
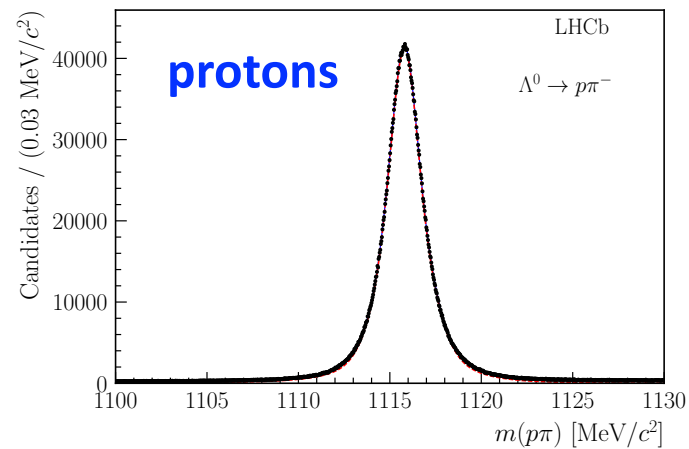
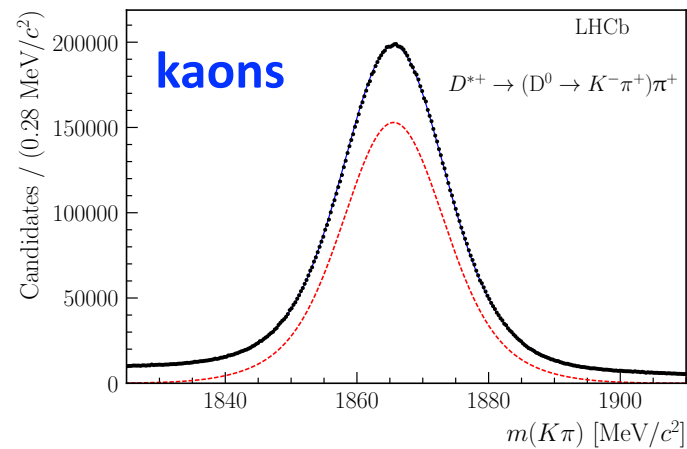
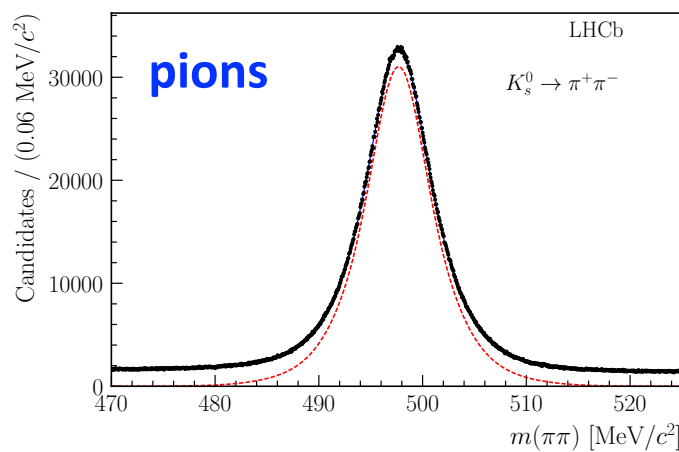
tracking system
 $\sigma_p/p = 0.5...1.0\%$

$$\frac{\sigma_E}{E} \sim \frac{10\%}{\sqrt{E}} \oplus 1\%$$

ECAL

Rare decays: background control is crucial

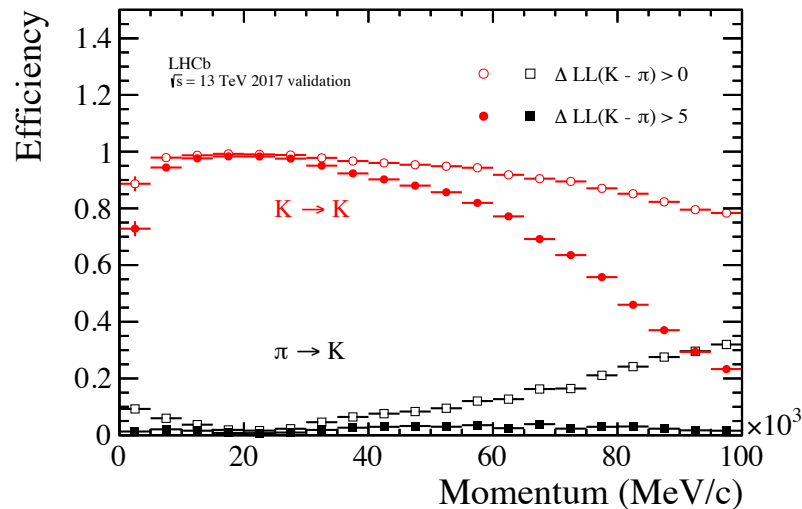
- Large calibration samples are collected with dedicated triggers and used for:
 - calibration of PID algorithms to correct MC simulation for data/MC differences
 - measurements of misidentification rates for data-driven estimates of peaking backgrounds



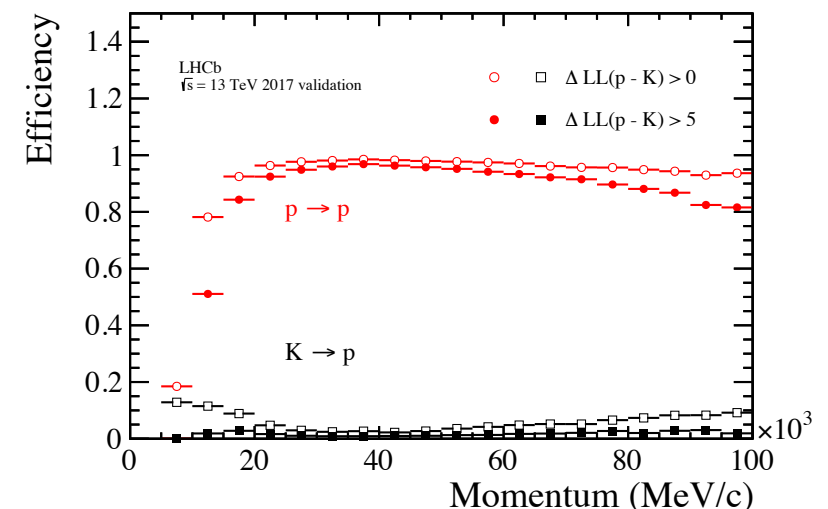
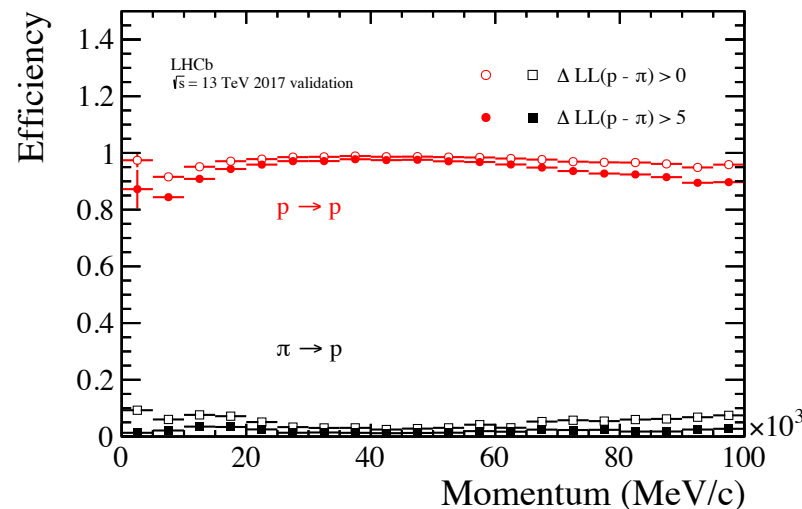
Performance of charged hadrons identification

- Very good discrimination power over wide kinematic ranges for hadrons:

kaons



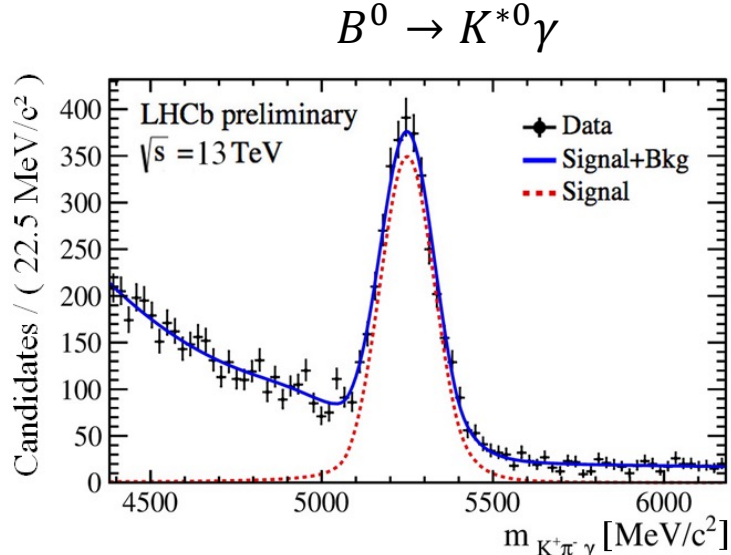
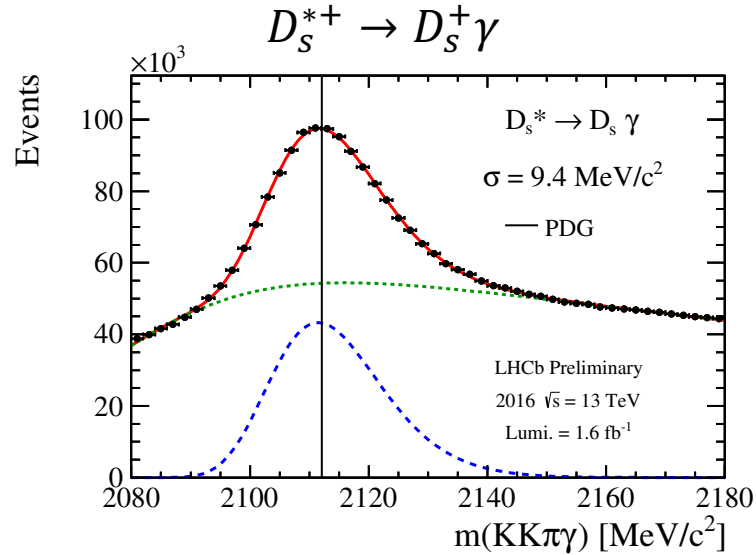
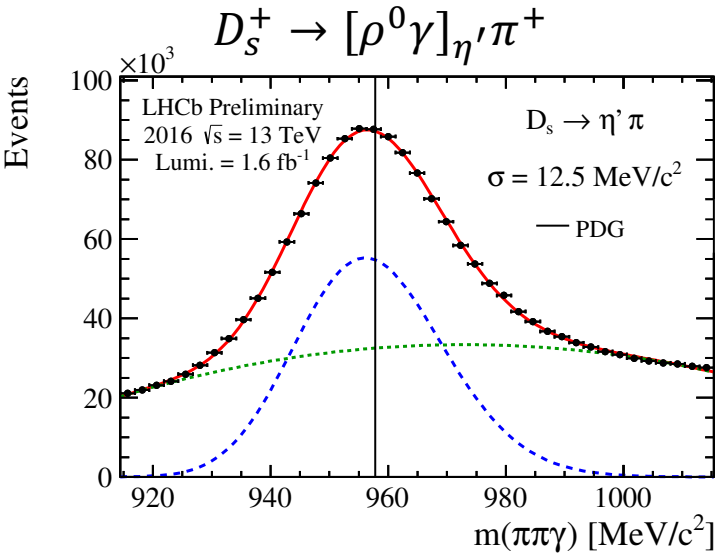
protons



Neutral calibration samples

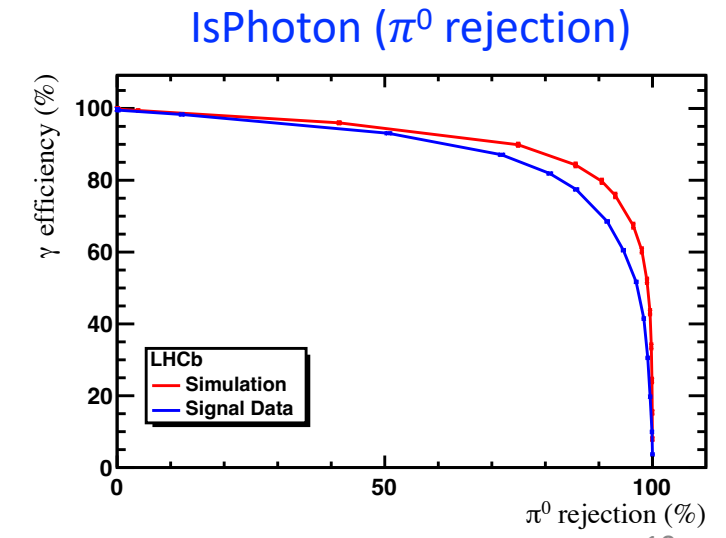
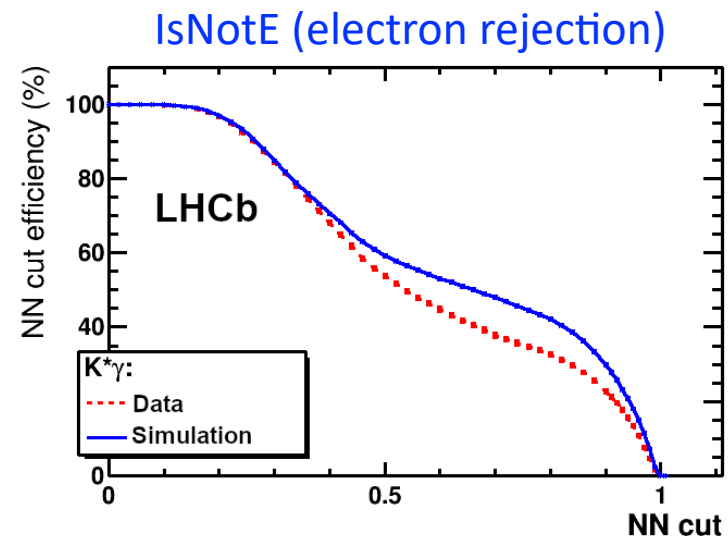
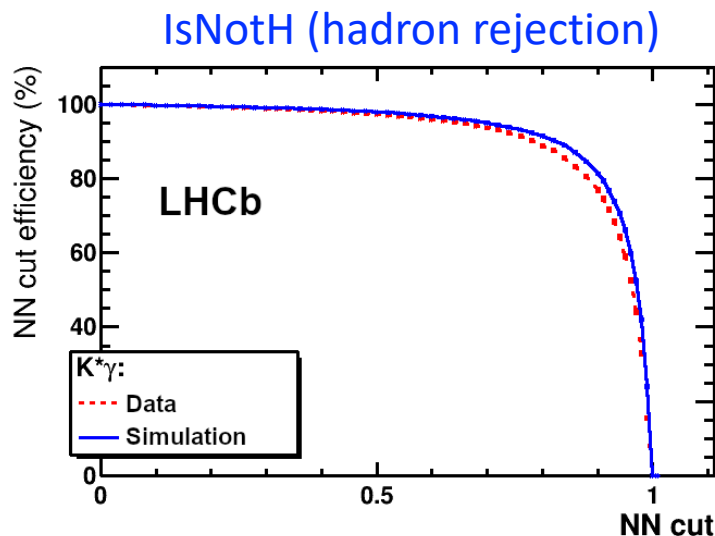
- multivariate classifiers combine variables describing energy deposits in the calorimeter subdetectors
- discriminate photons from hadrons, electrons and high-energy neutral pions

photons



Performance of photon identification

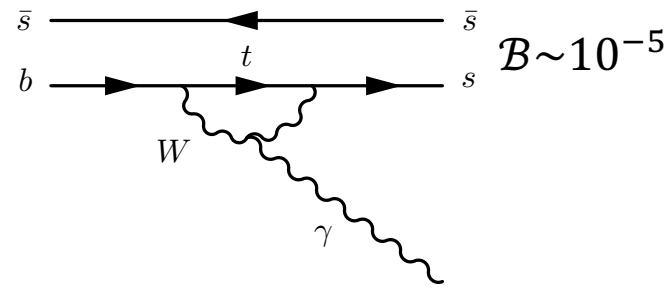
- Three different neural networks trained with simulation to separate photon signatures from other species:
 - γ vs. hadron: IsNotH
 - γ vs. e^+e^- : IsNotE
 - γ vs. π^0 : IsPhoton
- **Signal**: reconstructed photon candidates matching the generated photons ($B^0 \rightarrow K^{*0}\gamma$)
- **Background**:
 - electrons: reconstructed photons matching generated electrons ($B^0 \rightarrow K^{*0}e^+e^-$)
 - non-electromagnetic: reconstructed photons not matching to photon or electrons



The list of new results presented today:

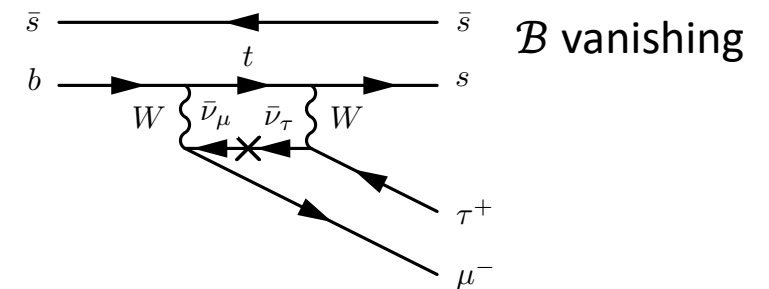
- **Amplitude analysis of the radiative $B_s^0 \rightarrow K^+ K^- \gamma$ decay**

- LHCb-PAPER-2024-002 in preparation
- *shown for the first time*



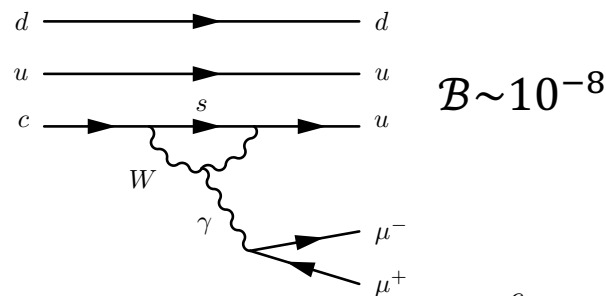
- **Search for the lepton-flavor violating decay $B_s^0 \rightarrow \phi \mu^\pm \tau^\mp$**

- LHCb-PAPER-2024-006 in preparation
- *shown for the first time*



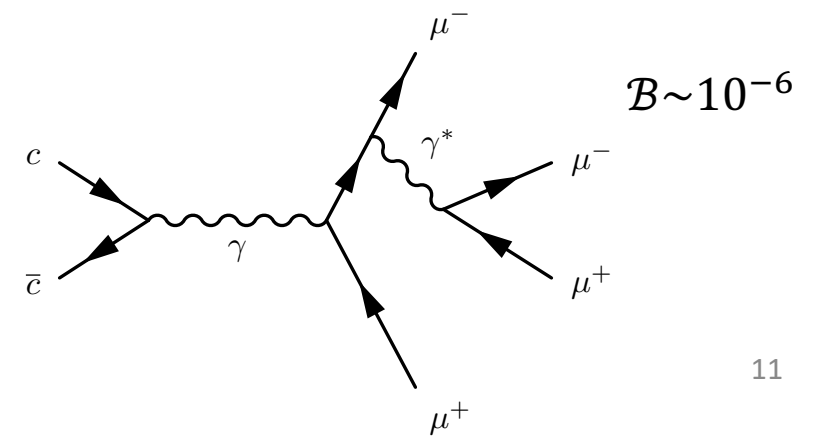
- **Search for the rare $\Lambda_c^+ \rightarrow p \mu^+ \mu^-$ decay**

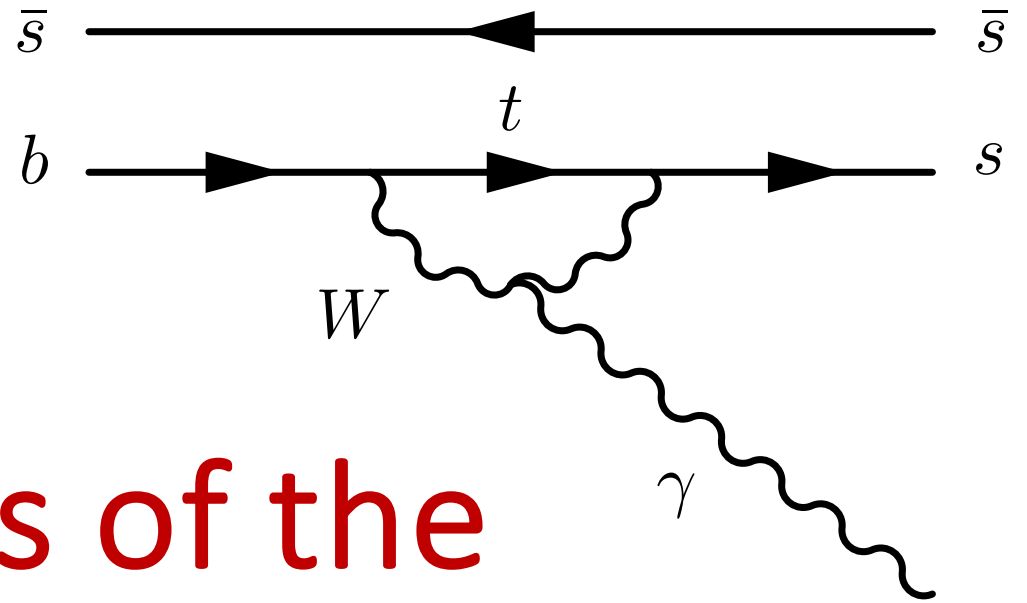
- LHCb-PAPER-2024-005 in preparation
- *shown for the first time*



- **Study of the rare decay $J/\psi \rightarrow \mu^+ \mu^- \mu^+ \mu^-$**

- [LHCb-CONF-2024-001](#)
- *new*

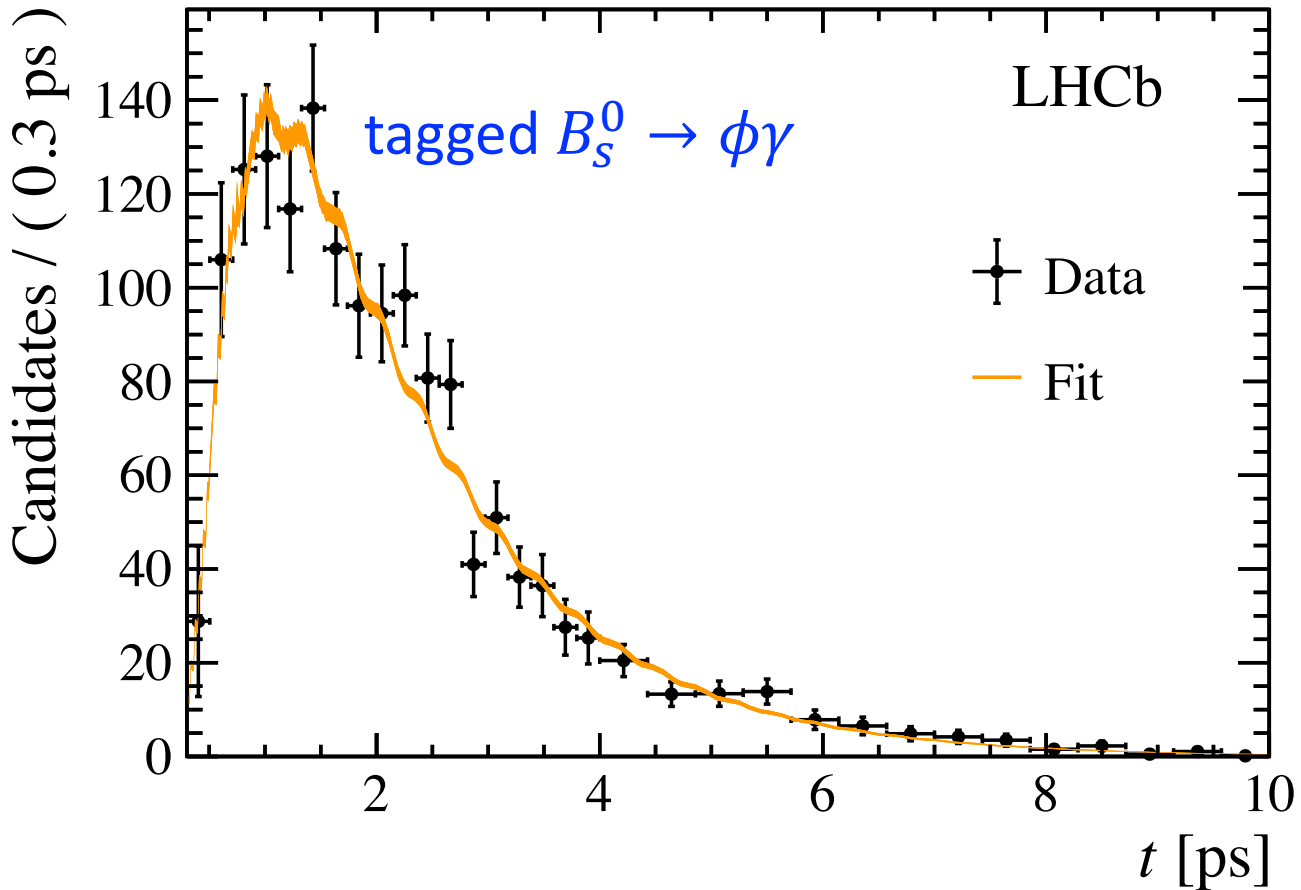




Amplitude analysis of the radiative $B_s^0 \rightarrow K^+ K^- \gamma$ decay

LHCb-PAPER-2024-002 in preparation

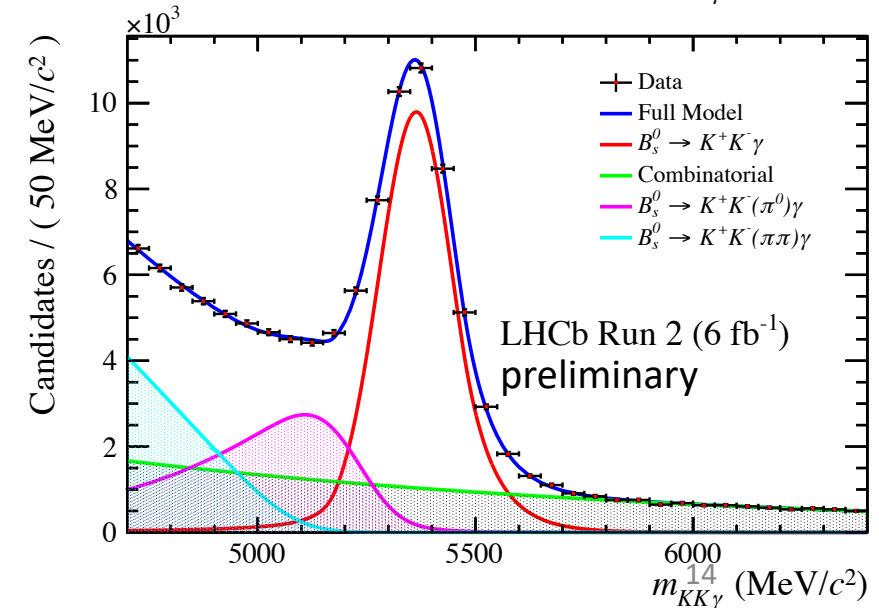
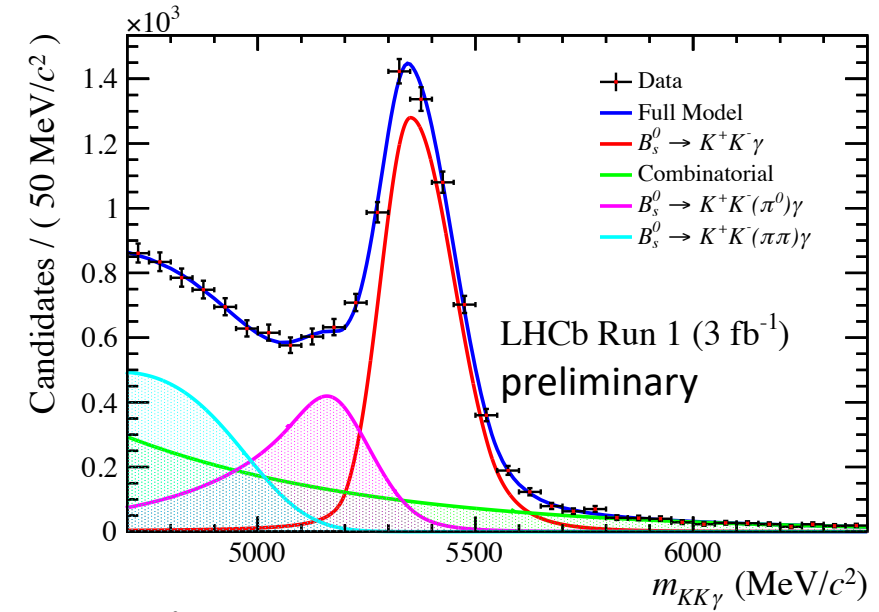
Exploring radiative B_s^0 decays



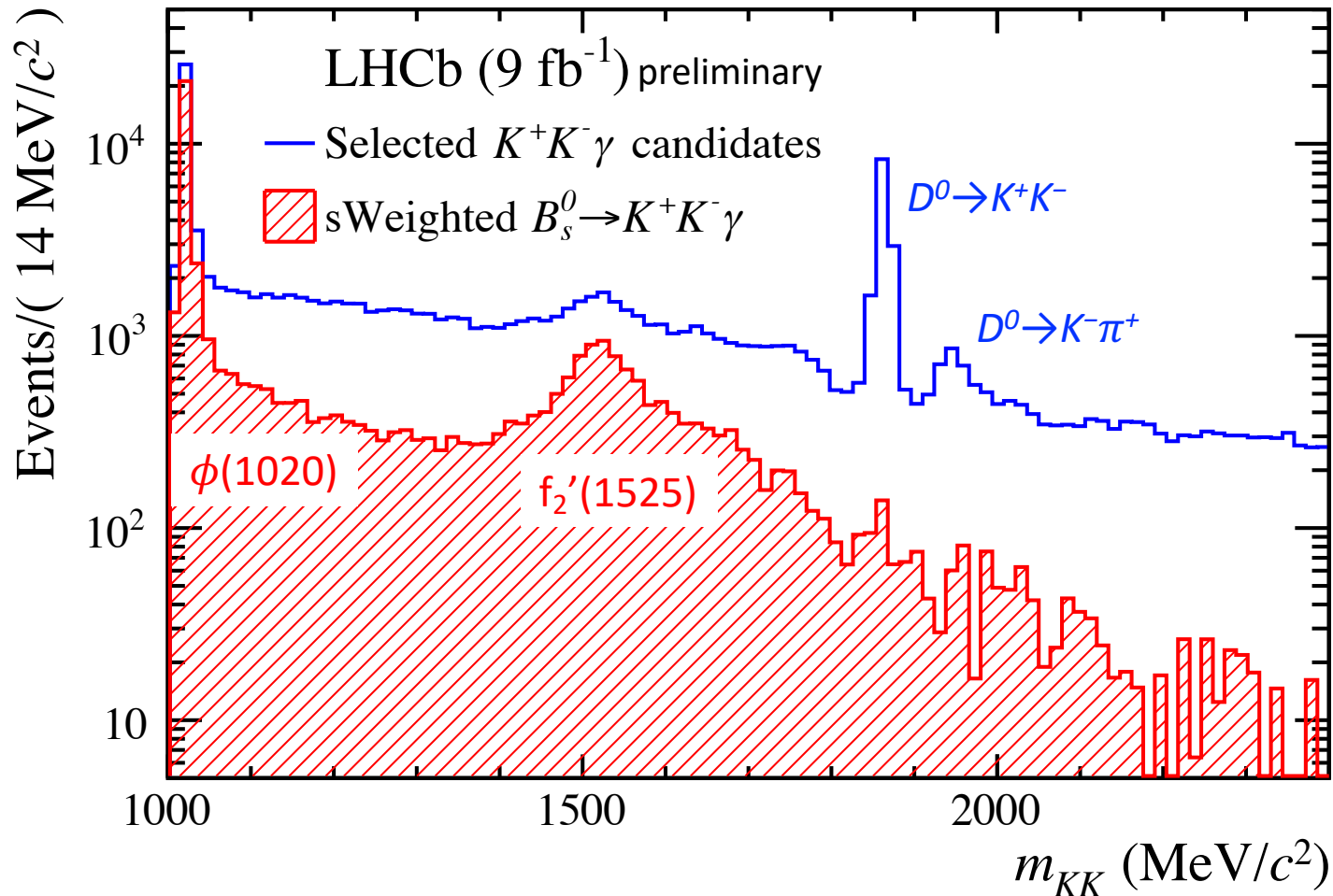
- $B_s^0 \rightarrow \phi \gamma$ is one of the few decays giving access to photon polarization measurement
- both tagged and untagged analyses performed by LHCb:
 - $\sim 1.5 - 2\sigma$ compatibility with the SM
- what about other contributions to $B_s^0 \rightarrow K^+ K^- \gamma$?

$B_s^0 \rightarrow K^+ K^- \gamma$ selection and fit

- Overcoming challenges:
 - resolution dominated by ECAL: $\sigma(m_{KK\gamma}) \approx 85$ MeV
 - photon trigger: $p_T(\gamma) > 3$ GeV
 - dedicated γ/π^0 separation criteria in photon ID
 - kaon ID to suppress $p \leftrightarrow K$ and $\pi^\pm \leftrightarrow K^\pm$ misID
 - anti-charm veto to reject $K^\pm h^0$ from $D_{(s)}$ decays:
 - $m(K^\pm \gamma (\leftrightarrow \pi^0)) > 2$ GeV
 - multivariate selection to suppress combinatorial bkg
- Mass fit strategy includes:
 - **signal**
 - **processes with one** and **two missing pions**
 - **combinatorial bkg**
 - **no peaking bkg ($Kh\gamma$, $Kh\pi^0$):** embedded into signal and accounted for in the amplitude analysis:
 - $B^0 \rightarrow (K\pi)\gamma$: $(4.5 \pm 1.1)\%$ and $\Lambda_b \rightarrow (pK)\gamma$: $(6.1 \pm 1.1)\%$



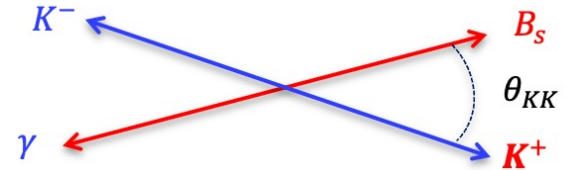
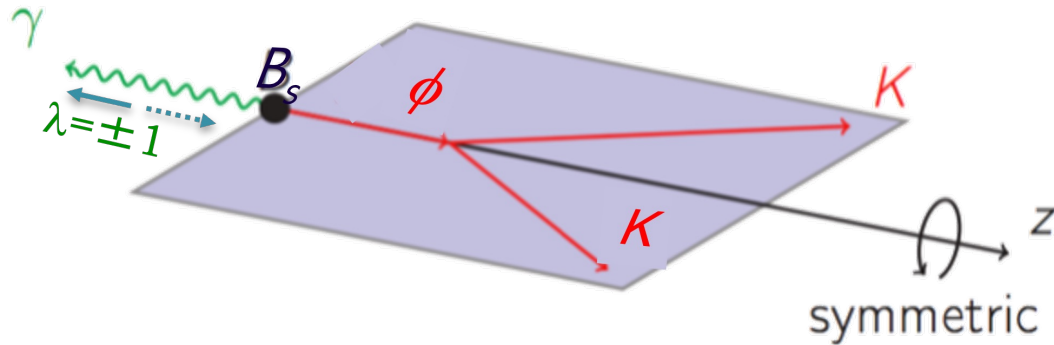
Extracted signal events



- statistical background subtraction is used to extract signal
- amplitude analysis is performed in the following KK mass ranges:
 - $[2m_K, 2400 \text{ MeV}]$, Run 2
 - $[2m_K, 1950 \text{ MeV}]$, Run 1

$B_s^0 \rightarrow K^+ K^- \gamma$: decay dynamics

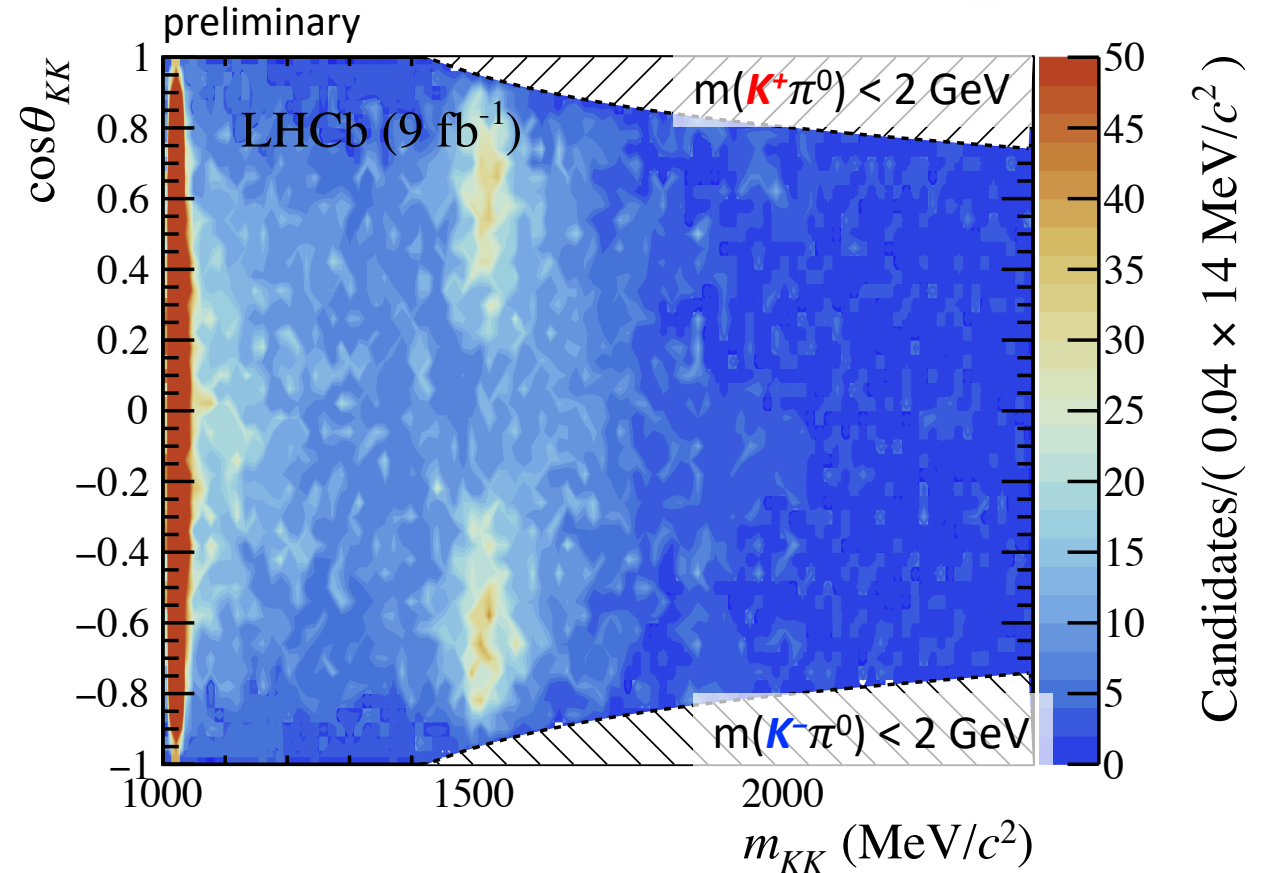
Symmetric decay:



- undetermined azimuthal angle integrated out as well as time-dependencies
- decay dynamics completely described with m_{KK} and helicity angle θ_{KK} :

$$\cos\theta_{KK} = \frac{(s_{K^+\gamma} - s_{K^-\gamma})m_{KK}}{4M_{B_s}q_Rq_{B_s}}$$

(definitions in the extra slides)



Amplitude model: (m_{KK}, θ_{KK}) PDF

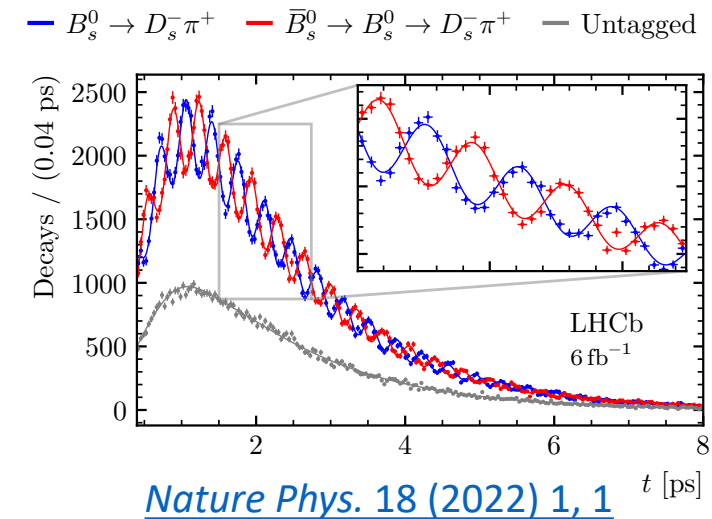
- Global PDF: $\mathcal{P}(m_{KK}, \theta_{KK}) = \mathcal{N}_s \mathcal{P}_s + \sum_{bkg} \mathcal{N}_{bkg} \mathcal{P}_{bkg}$
signal peaking backgrounds
- Signal PDF:
 - fast B_s oscillations \Rightarrow decay rate asymmetry is negligible and no expected CP asymmetry
 - interferences between odd- and even-spin components in the average cancel out
 - isobar model in the folded helicity semiplane $(m_{KK}, |\cos \theta_{KK}|)$ summing incoherently odd- and even-spin components:

- $\mathcal{P}(m_{KK}, \theta_{KK}) = \varepsilon(m_{KK}, |\cos \theta_{KK}|) \cdot \mathcal{J}_3(m_{KK}) \sum_{P=+,-} |\sum_{RP} C_{RP} \cdot \mathcal{A}_{RP}(m_{KK}, |\cos \theta_{KK}|)|^2$

- $\mathcal{A}_R(m_{KK}, |\cos \theta_{KK}|) = BW_R(m_{KK}) \cdot d_{10}^{JR}(\theta_{KK})$

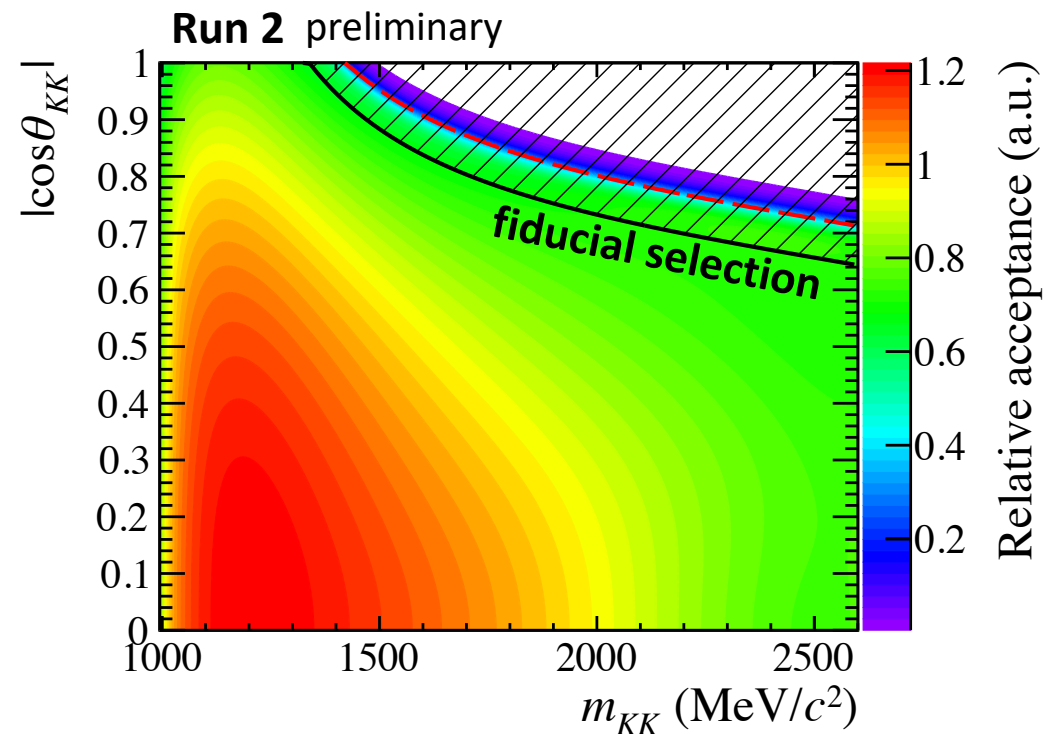
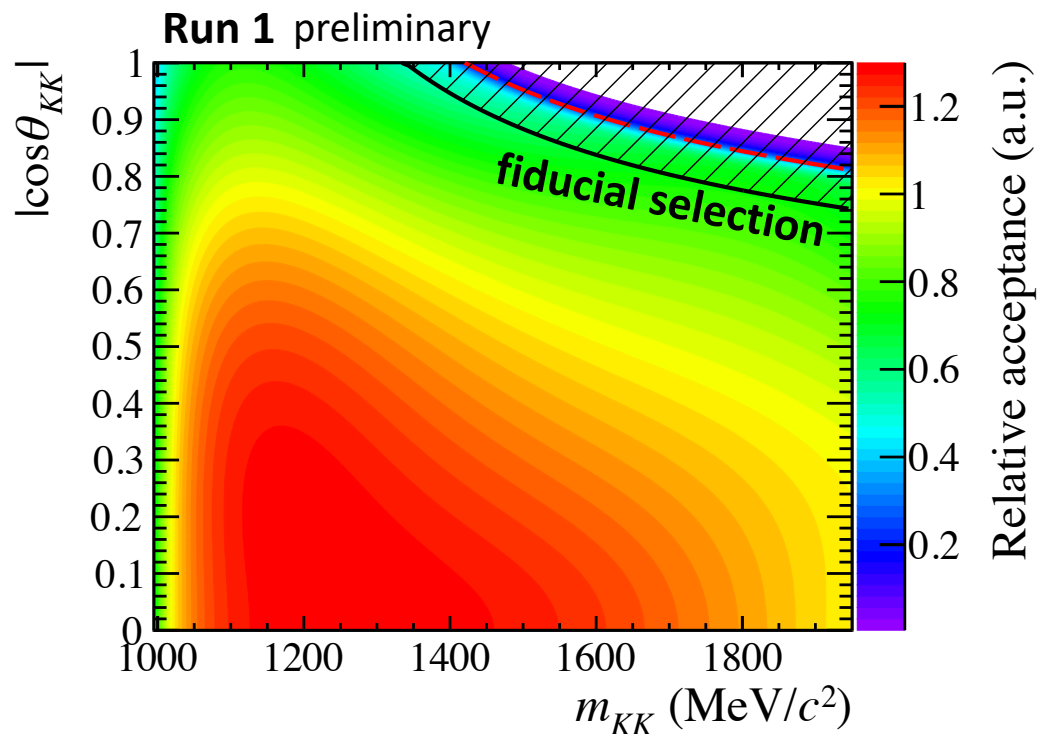
- m_{KK} resolutions included in the relativistic BW using analytical convolution

[[J.Math.Anal.Appl. 463 \(2018\) 2, 1040](#)]



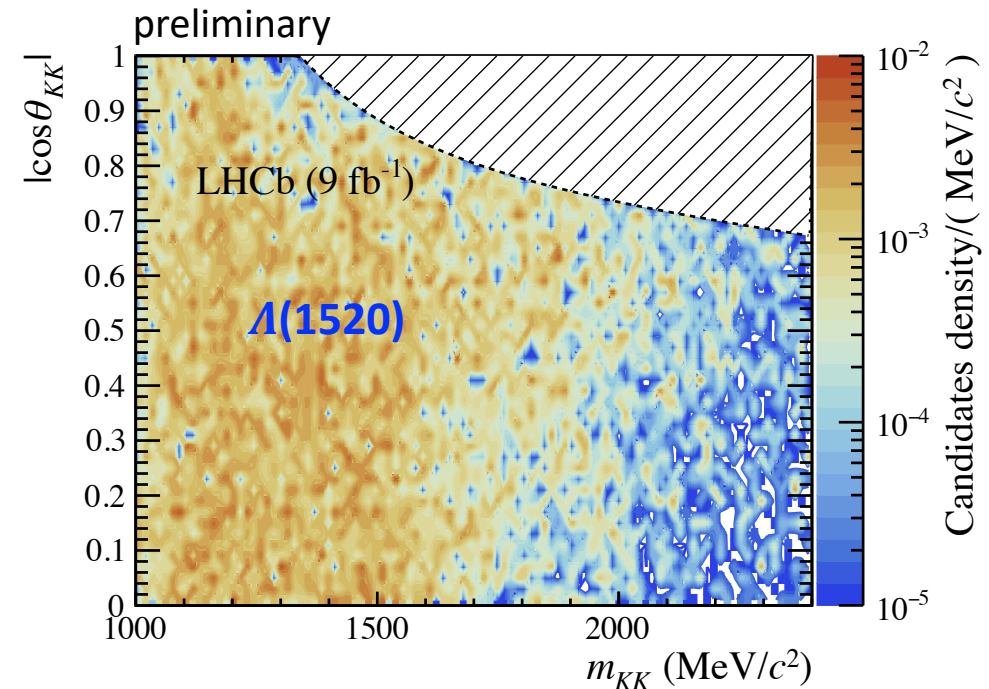
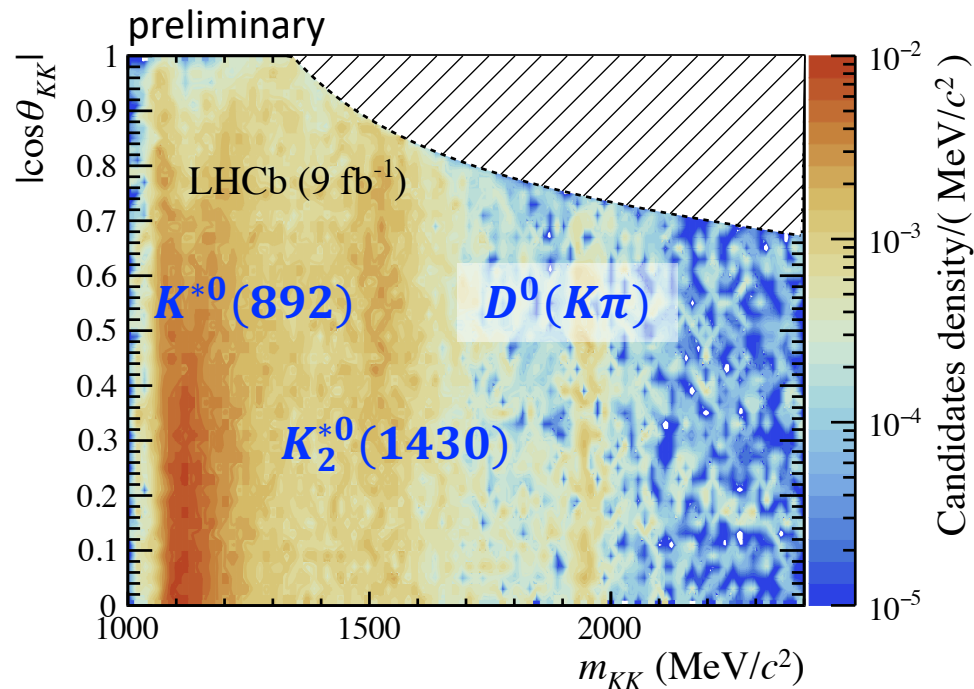
Acceptance: $\varepsilon(m_{KK}, \theta_{KK})$ 2D function

- Parameterised 2D acceptance based on Bernstein polynomials
- Anti-charm veto \Rightarrow mass-dependent helicity range
- Fiducial selection to avoid modelling resolution at the threshold (1% of events)



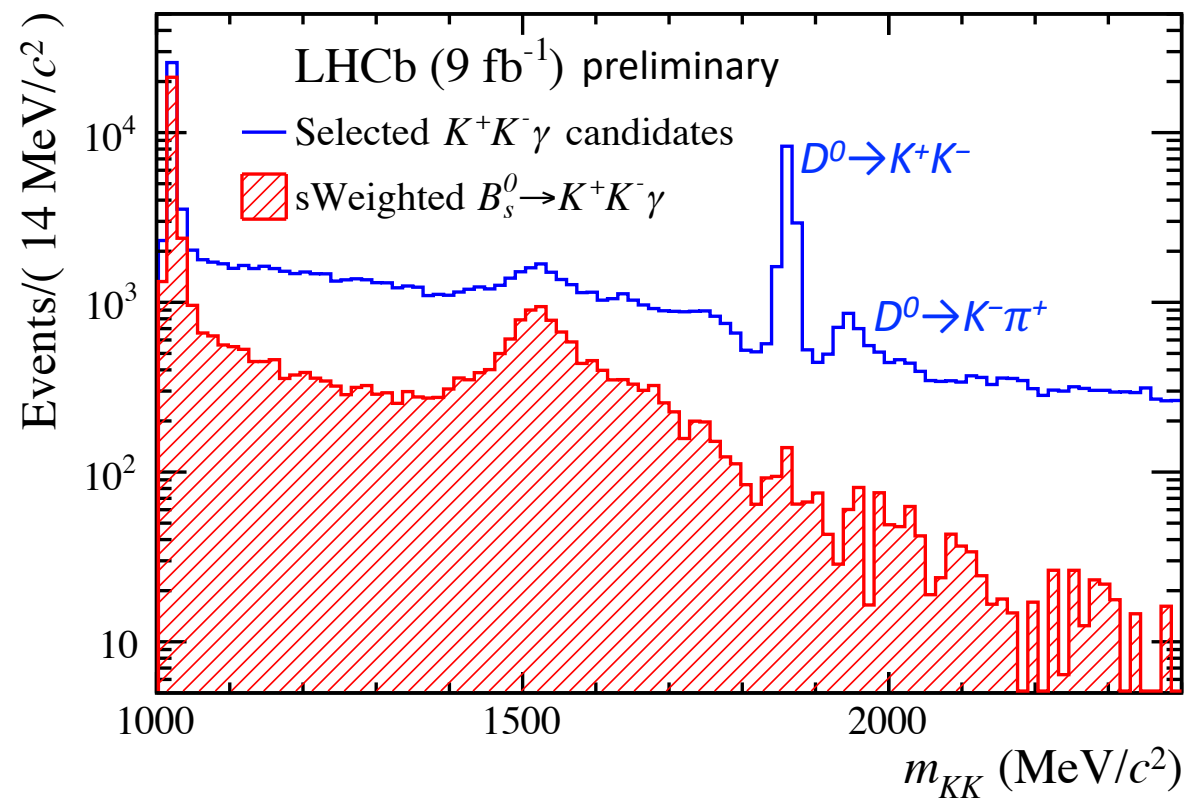
Peaking backgrounds model

- Consider only the dominant peaking backgrounds:
 - $B^0 \rightarrow (K\pi \rightarrow K)\gamma$ misID and $\Lambda_b \rightarrow (Kp \rightarrow K)\gamma$ misID
 - extract from control samples in data with $\pi \rightarrow K$ or $p \rightarrow K$ substitution
- PID reweighting performed using measured misID rates in control samples
- BDT acceptance reweighting based on MC simulation



Unsubtracted background: $D^0(K^+K^-)\pi^0$

- $D^0(K^+K^-)$ mostly populates the combinatorial and partially reconstructed background regions
 - small contamination in the signal region at the per mille level
 - m_{KK} PDF is extracted from mass sidebands – no angular dependency, flat helicity contribution is used
- $D^0(K\pi)\pi^0$ is included into $K\pi\gamma$ background
- other possible ($KK\pi^0$) contamination from charmless B decays is expected to be small and is treated in systematic uncertainties

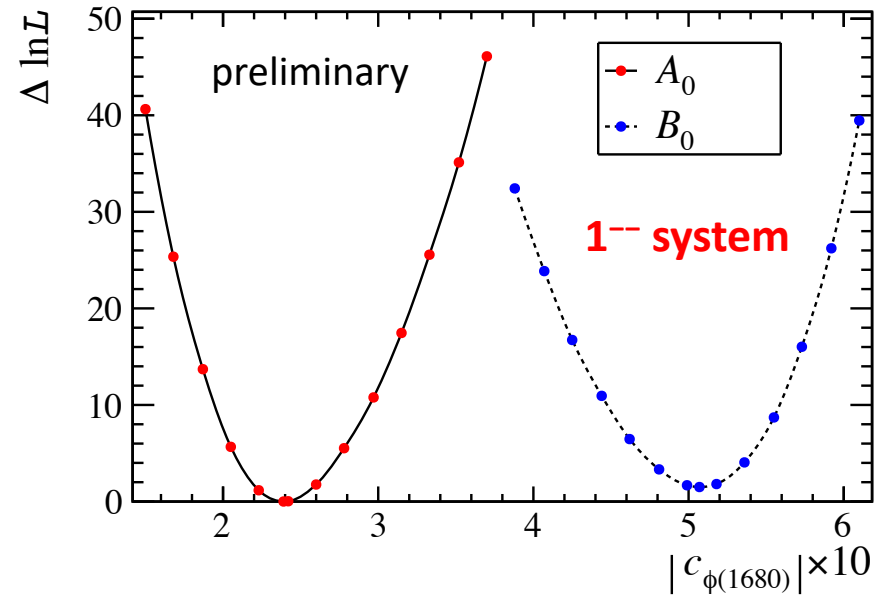
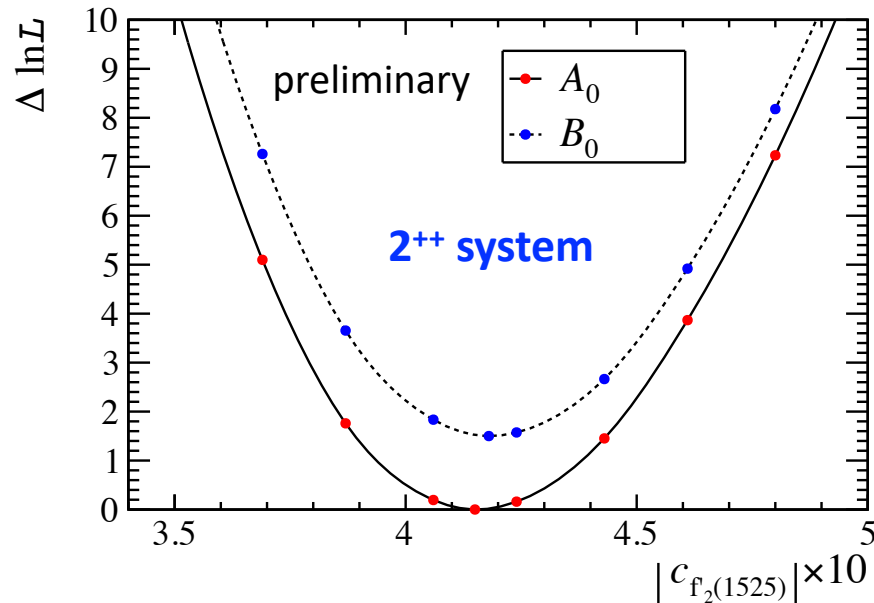


Main model results

- Well-established dikaon states lead to large $\Delta\ln\mathcal{L}$ gain (>12.5 , corresponding to 5σ significance) and with $|c_R|$ isobar significance larger than 3σ
- Nonresonant (NR): P-wave uniformly distributed in mass with constant phase
- Several distinct tensor candidates around 2 GeV give similar significance

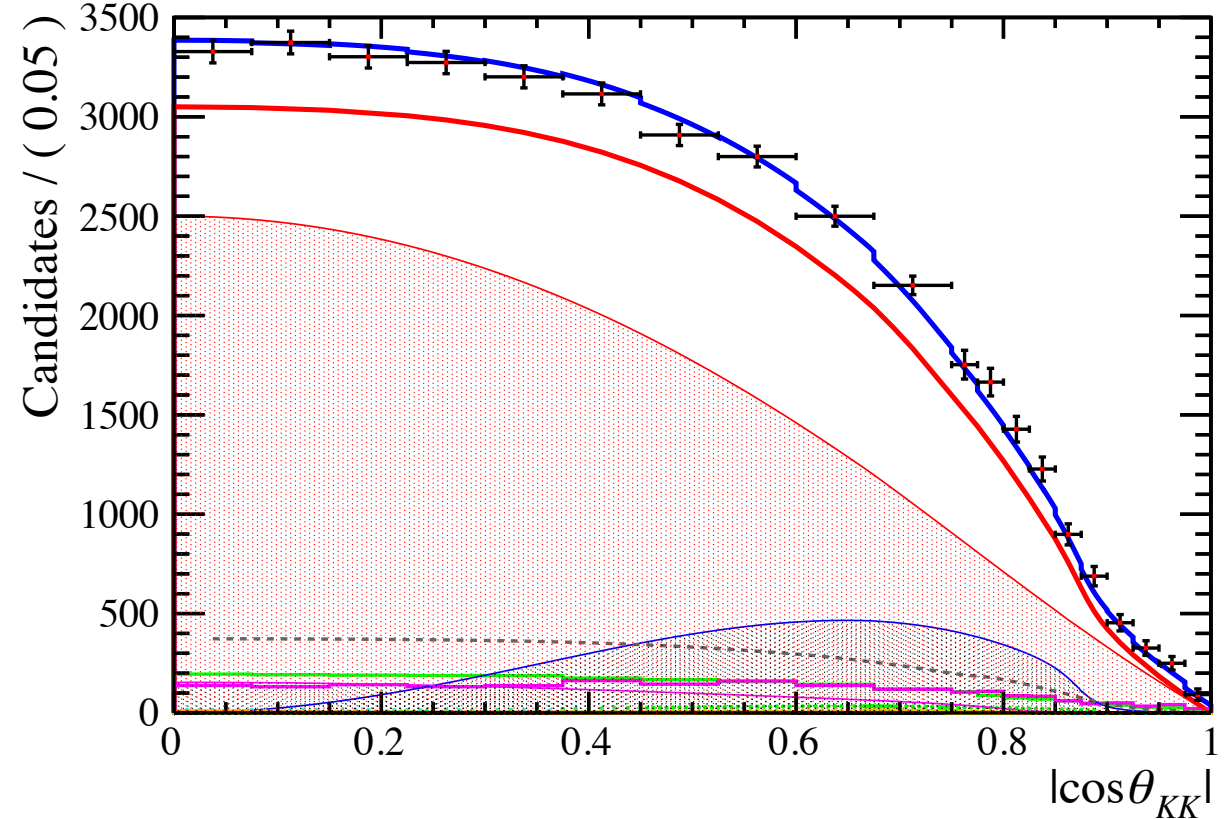
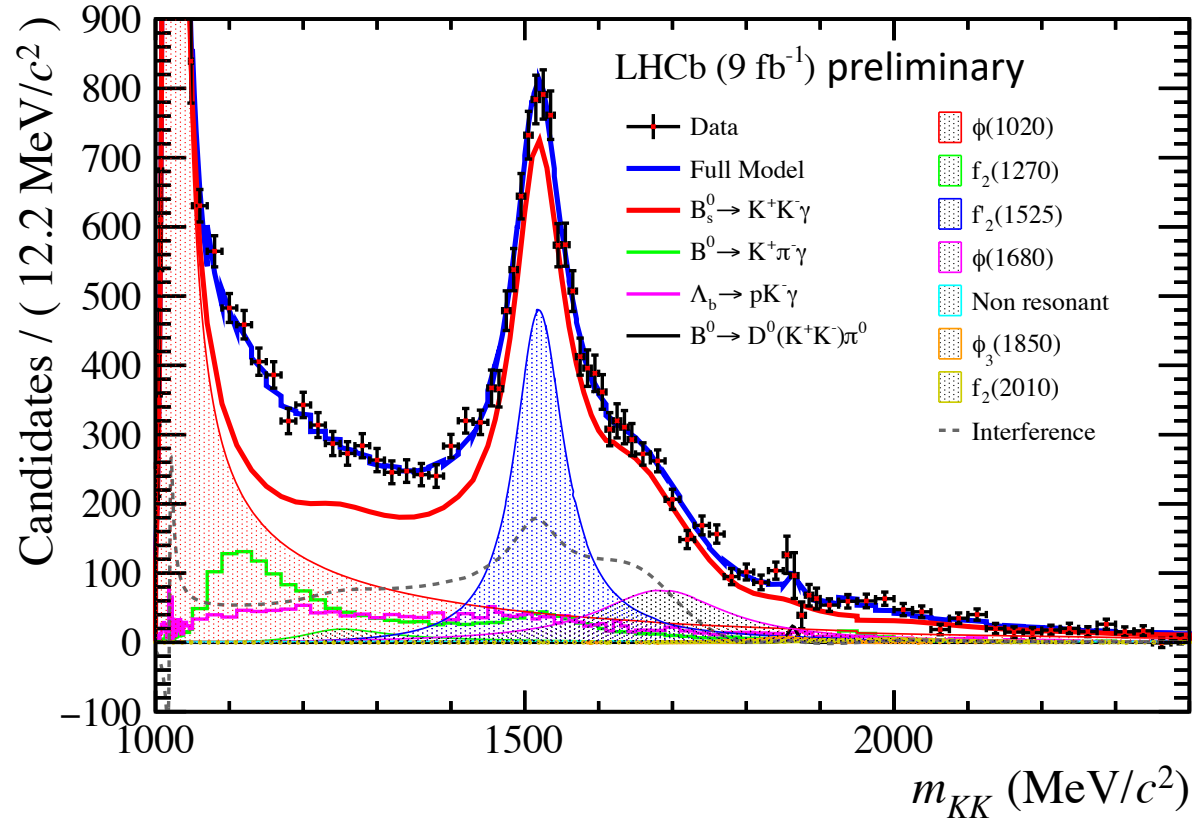
State	J^{PC}	μ_R (MeV/ c^2)	Γ_R (MeV)	$\mathcal{B}_{K^+K^-}$ (%)	$ c_R $ ($\times 10$)	$(\chi^2_{ c_R })$	$\Delta\ln\mathcal{L}$
$\phi(1020)$	1^{--}	1019.461 ± 0.016	4.249 ± 0.013	49.2 ± 0.5	10 (fix)	-	-
$f'_2(1525)$	2^{++}	1517.4 ± 2.5	86 ± 5	43.8 ± 1.1	4.16 ± 0.09	(2270)	-
$\phi(1680)$	1^{--}	1689 ± 12 (*)	211 ± 24 (*)	seen	2.40 ± 0.15	(266)	+304
$f_2(1270)$	2^{++}	1275.5 ± 0.8	$186.6^{+2.2}_{-2.5}$	$2.30^{+0.25}_{-0.20}$	1.07 ± 0.17	(41)	+18
$\phi_3(1850)$	3^{--}	1854 ± 7	87^{+28}_{-23}	seen	0.61 ± 0.16	(14)	+15
$f_2(2010)$	2^{++}	2011^{+62}_{-76}	202^{+67}_{-62}	seen	0.74 ± 0.18	(16)	+13
$(\text{KK})_{\text{NR}}$	1^{--}	-	-	-	0.79 ± 0.26	(10)	+17

Likelihood minima pattern



- several quasi-degenerate solutions within $\Delta LL < 3$ due to weakly constrained interference pattern:
 - the odd and the even-spins form two incoherent subsystems
 - **2⁺⁺ system** (4-fold ambiguity): dominant $f_2'(1525)$ surrounded by two small components interfering positively or negatively
 - **1⁻⁻ system** (2-fold ambiguity): separated $\phi(1020)$ and $\phi(1680)$ interfering with NR component covering full phase space
- the preferred solution corresponds to the smallest fit-fractions along with positive interference for all components

Best fit projections



- $N(B_S^0) = (44.4 \pm 0.5) \times 10^3$, out of which about 2% have m_{KK} above 1.8 GeV

Summary

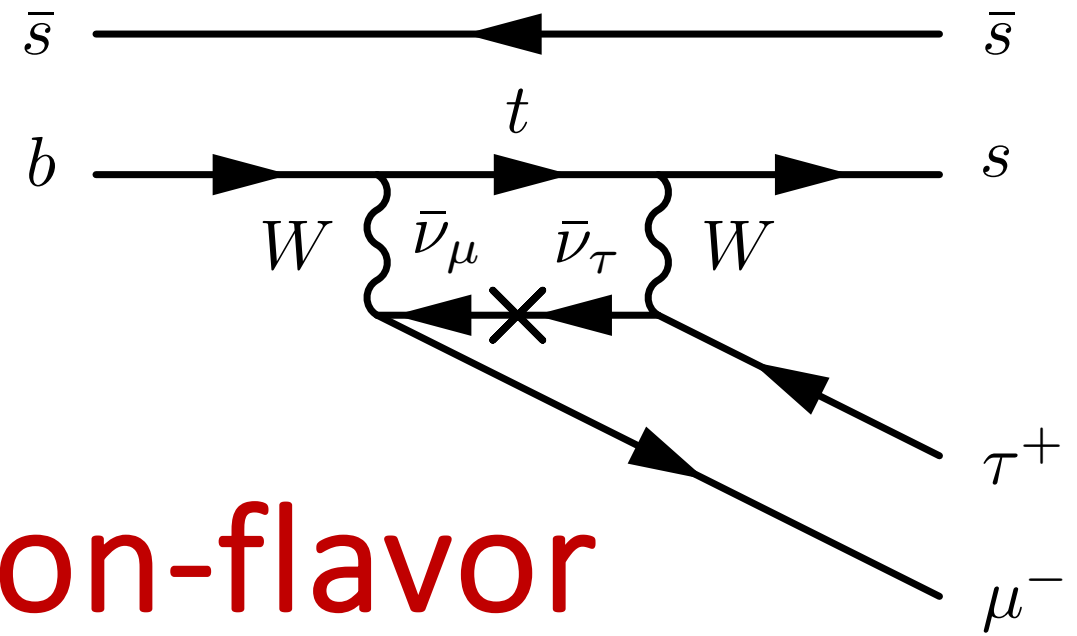
- considering possible contributions from $\{f_2'(1525), f_2(1270), f_2(2010)\}$, the overall tensor fit-fraction is

$$\mathcal{F}_{\{f_2\}} = 16.8 \pm 0.5 \text{ (stat)} \pm 0.7 \text{ (syst)}\%$$

- the decay $B_s^0 \rightarrow f_2'(1525)\gamma$ is observed for the first time ($\mathcal{B}(B_s^0 \rightarrow \phi\gamma) = 3.4 \times 10^{-5}$):

$$\frac{\mathcal{B}(B_s^0 \rightarrow f_2'\gamma)}{\mathcal{B}(B_s^0 \rightarrow \phi\gamma)} = 0.194_{-0.008}^{+0.009} \text{ (stat)}_{-0.005}^{+0.014} \text{ (syst)} \pm 0.005 \text{ (BR)}$$

- weak constraints on other isobars are also obtained
- mass and width for the $f_2'(1525)$ are measured in good agreement with the current world average and with the previous LHCb measurement



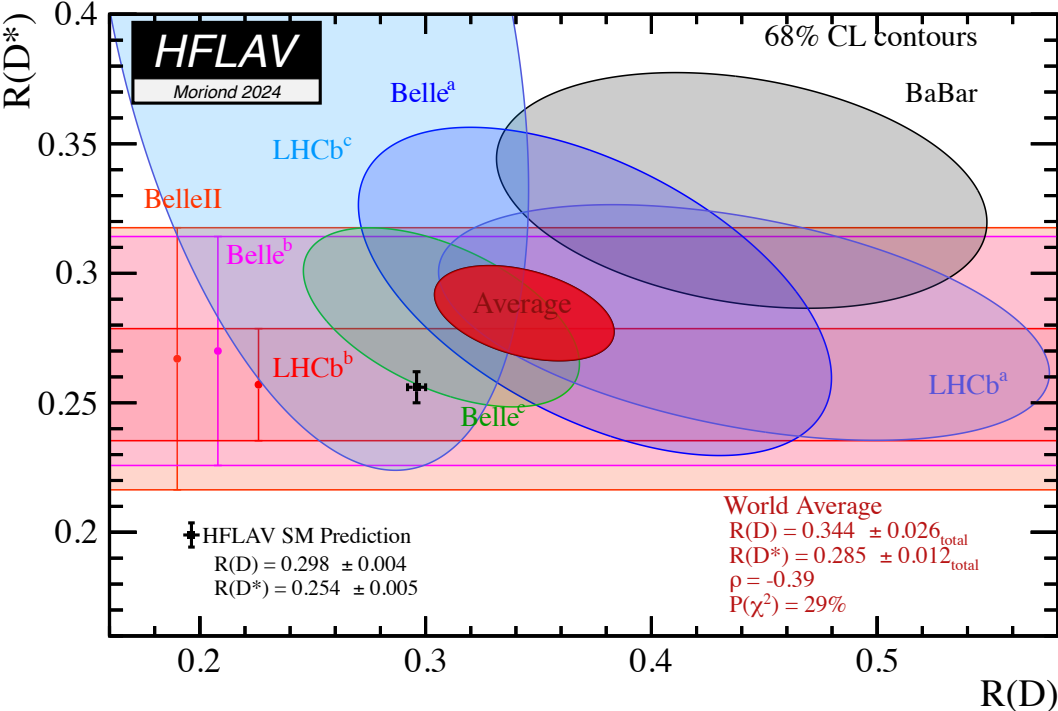
Search for the lepton-flavor violating decay $B_s^0 \rightarrow \phi \mu^\pm \tau^\mp$

LHCb-PAPER-2024-006 in preparation

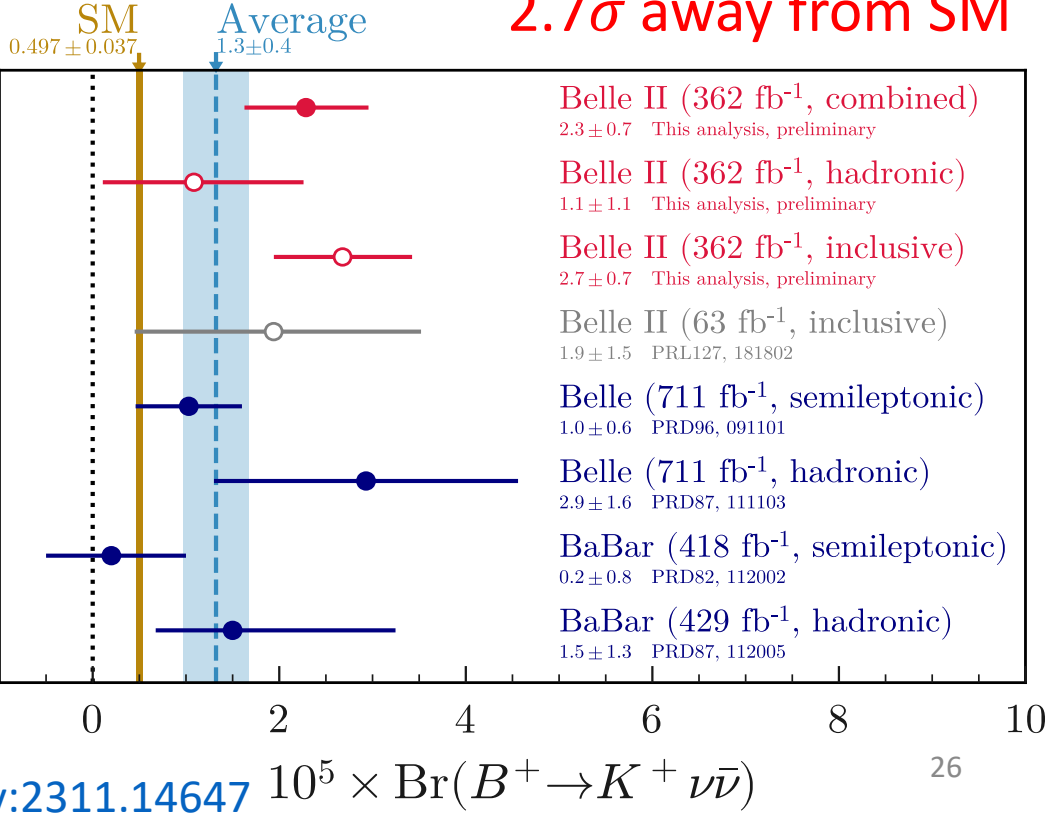
Motivation

- persisting anomalies in $R(D)$ and $R(D^*)$ and recent enhanced evidence for $B^+ \rightarrow K^+ \nu \bar{\nu}$ motivate BSM models leading to lepton-flavor-violating signatures

3.2 σ away from SM

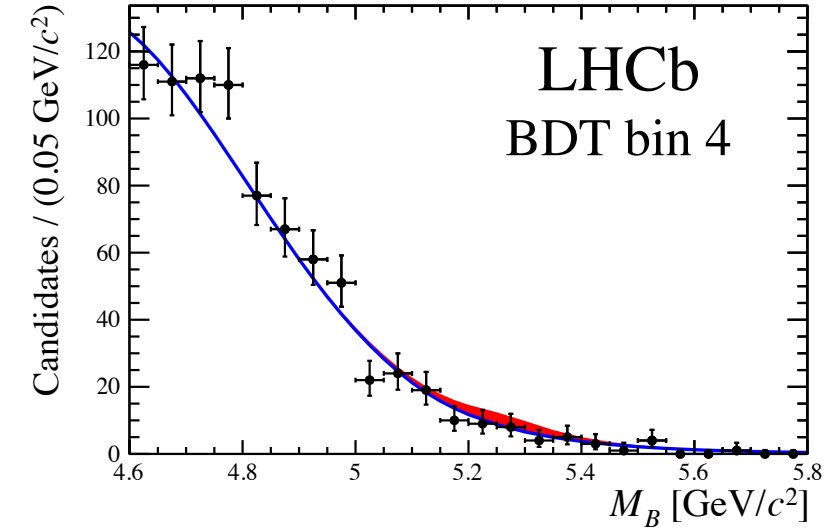


2.7 σ away from SM



Third lepton generation is tricky

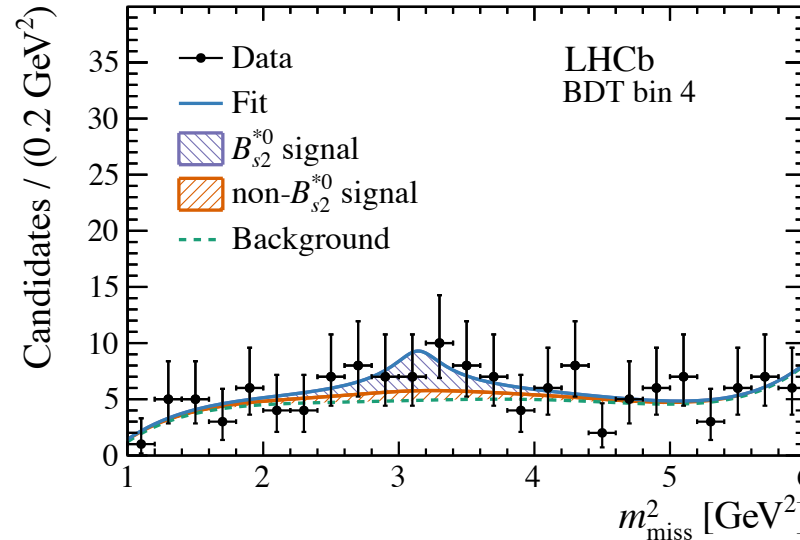
[Phys.Rev.Lett. 123 \(2019\) 211801](#)



$$\mathcal{B}(B_s^0 \rightarrow \tau\mu) < 4.2 \times 10^{-5} @ 95\% CL$$

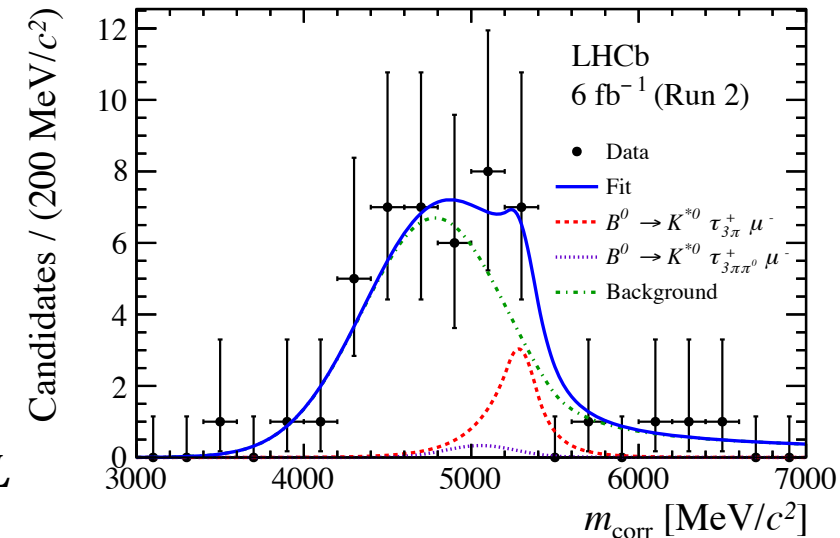
- Get penalized for visible τ decay modes with multiple tracks in the final state

[JHEP 06 \(2020\) 129](#)



$$\mathcal{B}(B^+ \rightarrow K^+\tau^+\mu^-) < 3.9 \times 10^{-5} @ 90\% CL$$

[JHEP 06 \(2023\) 143](#)



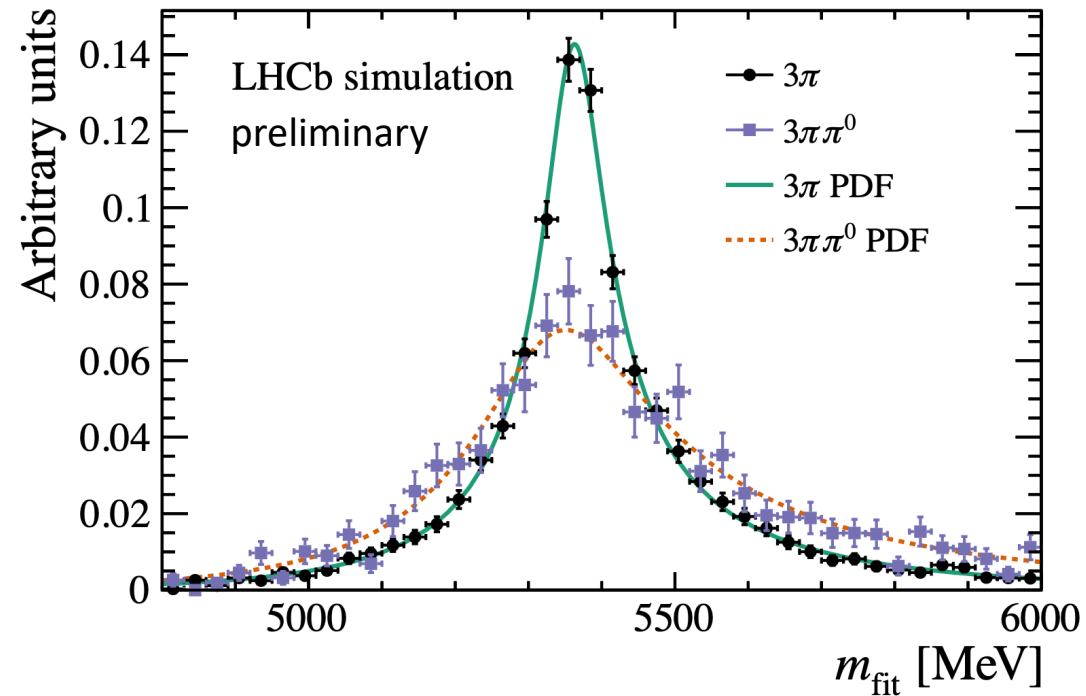
$$\mathcal{B}(B^0 \rightarrow K^{*0}\tau^+\mu^-) < 1.0 \times 10^{-5} @ 90\% CL$$

- For comparison, $\mathcal{B}(B^0 \rightarrow K^{*0}\mu^+e^-) < 5.7 \times 10^{-9} @ 90\% CL$

Analysis strategy

- B_S^0 is produced at low rate, but low background
- use $\tau \rightarrow 3\pi$ (including $\tau \rightarrow 3\pi\pi^0$) channel
- reconstruct B_S^0 mass using kinematic fit with vertex and mass constraints
- peaking misID background $B \rightarrow \bar{D}\phi\pi^+$ is estimated and included in the fit
- other backgrounds described in the fit with a smooth function
- normalization channel
 - $B_S^0 \rightarrow (\psi(2S) \rightarrow J/\psi\pi^+\pi^-)\phi$
 - difference in one particle: muon vs. pion

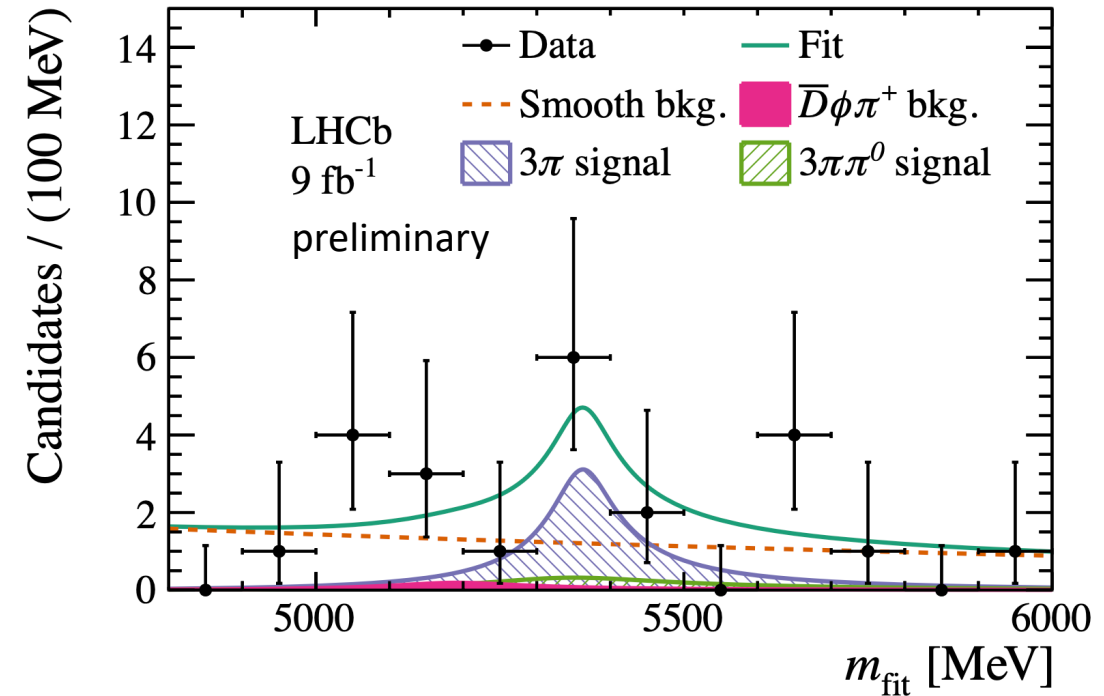
Signal extraction:
fit to a B_S^0 candidate mass



Backgrounds handling

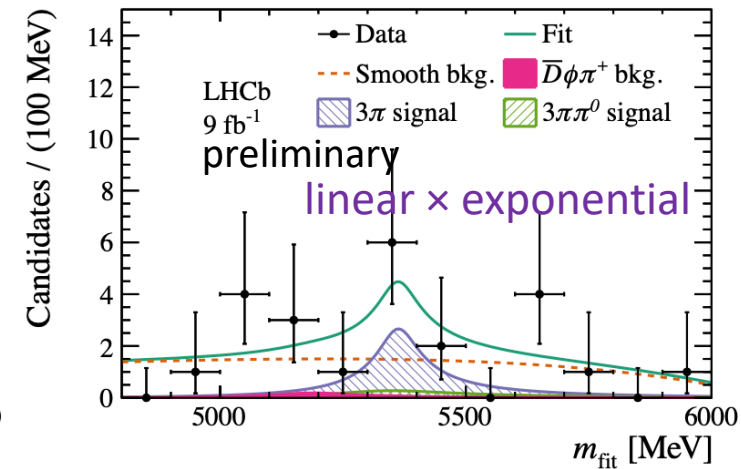
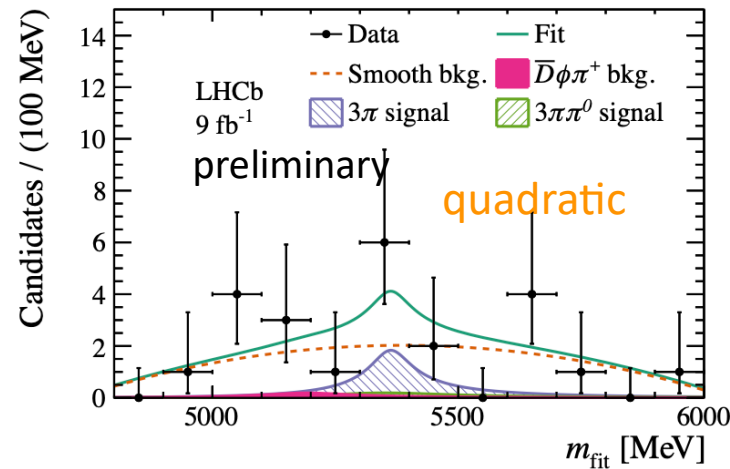
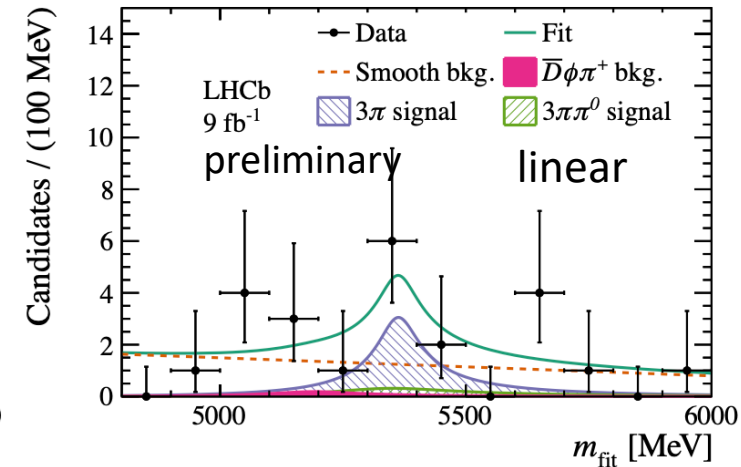
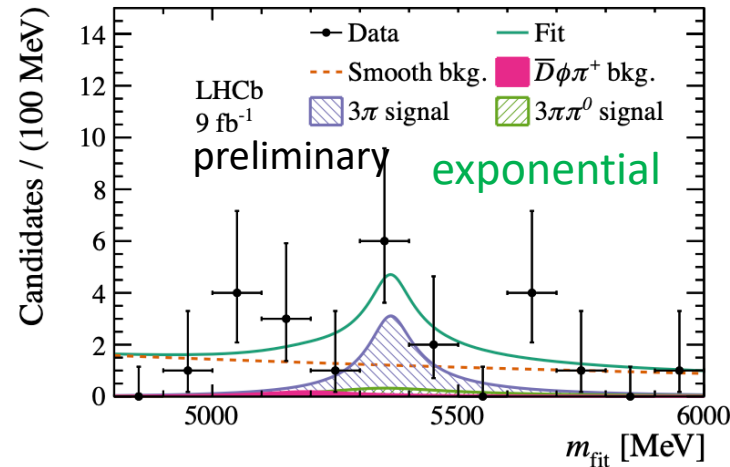
- **combinatorial background** is suppressed with a BDT trained on wrong-sign data sample as bkg proxy
- partially reconstructed background is suppressed with a BDT trained on low-mass sideband
- **misID background** is estimated with
 - control samples in data selecting $B \rightarrow \bar{D}\phi\pi^+$ with $\bar{D}^0 \rightarrow K^+\pi^-$, $D^- \rightarrow K^+\pi^-\pi^-$, $D_s^- \rightarrow K^+K^-\pi^-$
 - then extrapolate to signal region with $\pi \rightarrow \mu$ misID probabilities measured in data, $O(10^{-3})$
 - and ratios of $\bar{D} \rightarrow \pi^-\pi^+\pi^-X$ cocktail to exclusive modes from MC simulation, informed by BES III results

Charm meson	Control yield	Expected misid.
D^-	309 ± 31	0.11 ± 0.01
\bar{D}^0	343 ± 27	0.07 ± 0.01
D_s^-	632 ± 39	0.45 ± 0.03



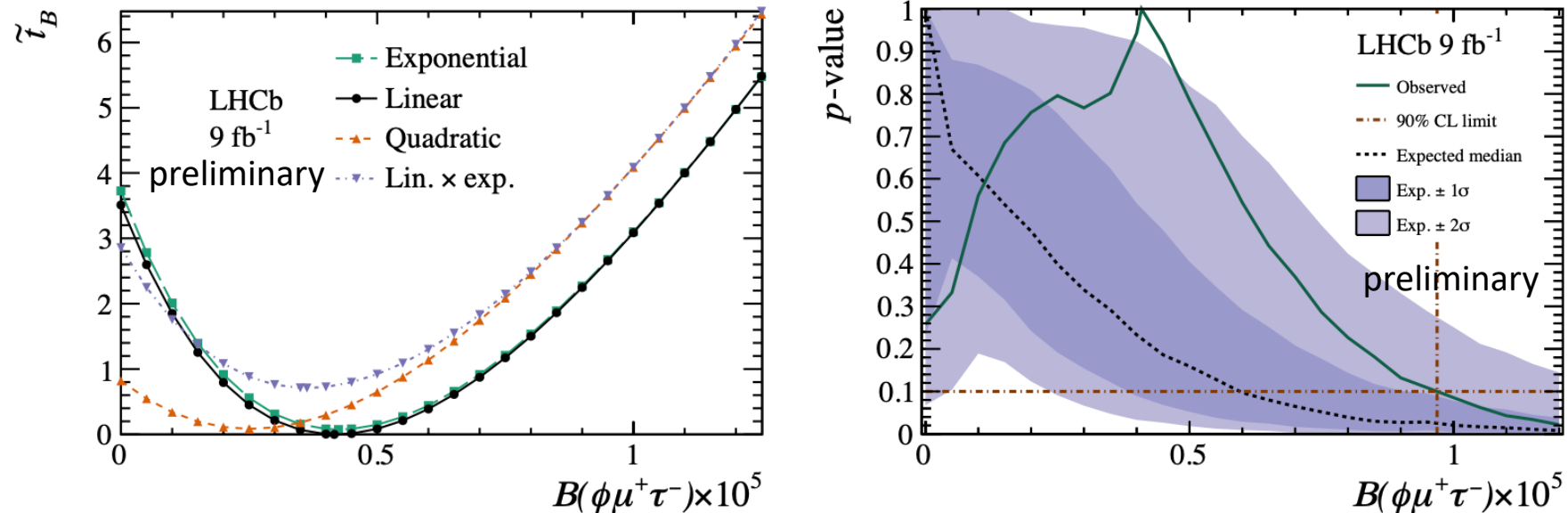
Final fit

- signal shapes are taken from MC simulation and are Gaussian-constrained
- misID background shape is Gaussian-constrained too
- remaining background is modelled with free to vary:
 - exponential
 - linear
 - quadratic
 - linear \times exponential
- signal is required to be non-negative



Results of the first search for this channel

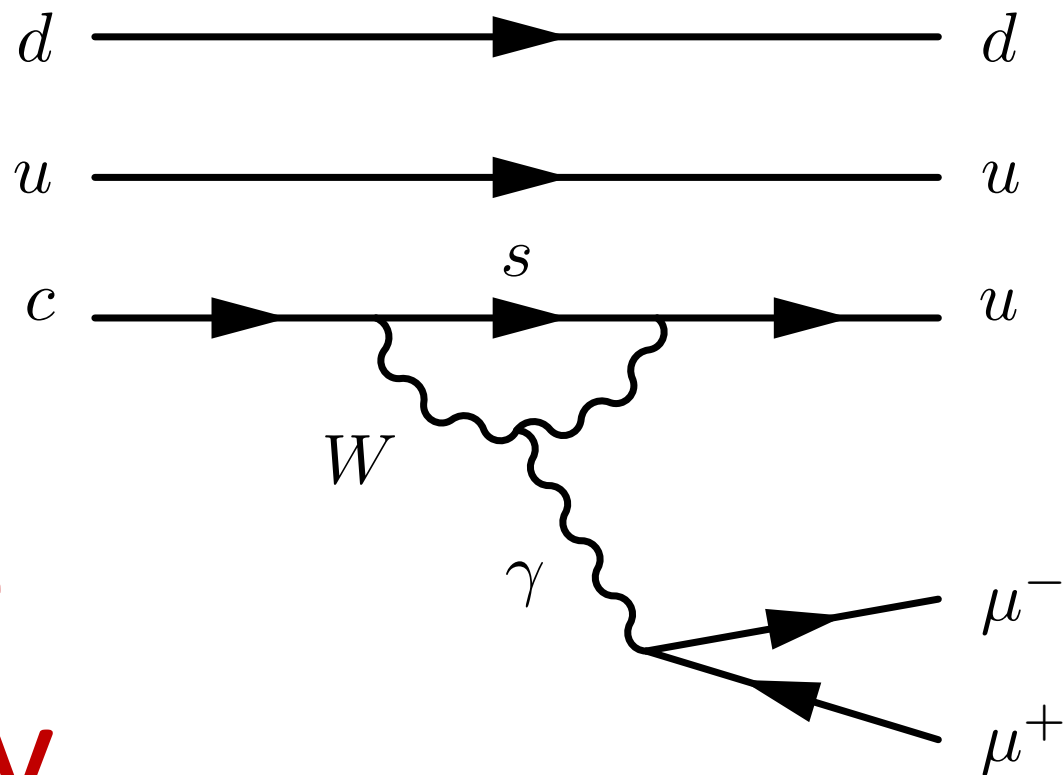
- the overall best fit uses the linear background model
- extracted BF is 4.1×10^{-6} with a local significance below 1.5σ



$$\mathcal{B}(B_s^0 \rightarrow \phi\mu^+\tau^-) < 1.0 \times 10^{-5} \text{ at 90\% CL,}$$
$$\mathcal{B}(B_s^0 \rightarrow \phi\mu^+\tau^-) < 1.1 \times 10^{-5} \text{ at 95\% CL.}$$

Search for the rare $\Lambda_c^+ \rightarrow p \mu^+ \mu^-$ decay

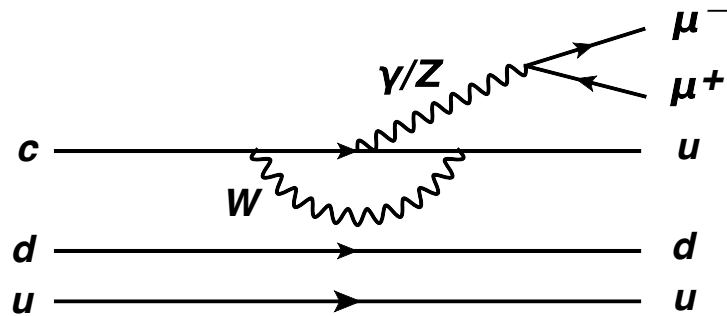
LHCb-PAPER-2024-005 in preparation



Motivation: GIM-suppressed charm penguins

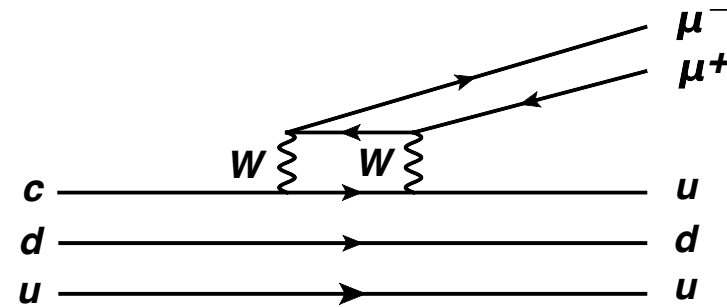
SM $\mathcal{B}(\Lambda_c^+ \rightarrow p\mu^+\mu^-)$:

- $\sim 10^{-8}$: short distance $c \rightarrow u\ell^+\ell^-$
- $\sim 10^{-6}$: long-distance enhancement (resonant)



Experimental status

- BaBar: $< 4.5 \times 10^{-5}$ @ 90% CL
- LHCb Run 1: $< 7.7 \times 10^{-8}$ @ 90% CL



Goals:

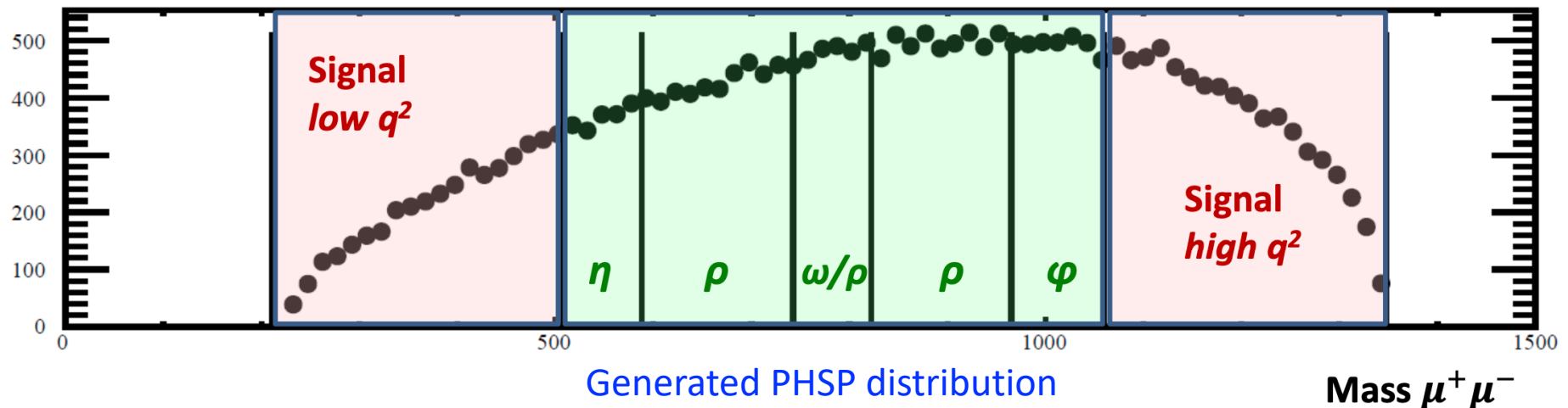
- search for rare decay $\Lambda_c^+ \rightarrow p\mu^+\mu^-$ in dimuon mass regions where resonant contribution is minimal
- branching fraction measurement in dimuon mass regions, dominated by η, ω, ρ

Signal regions

- BDT trained against combinatorial background, using
 - topological and kinematic variables and
 - vertex and isolation variables in addition
- backgrounds:
 - combinatorial, described with exponential
 - $\Lambda_c^+ \rightarrow p\pi^+\pi^-$, where pions misIDed as muons, described with shape from simulation
- final selection is optimized in 3D in (BDT response, proton ID and muon ID) by minimising UL on expected BF

Region	Range [MeV/c ²]
<i>low-m</i> region	$211.32 < m_{\mu^+\mu^-} < 507.86$
<i>high-m</i> region	$1059.46 < m_{\mu^+\mu^-} < 1348.13$
η region	$507.86 < m_{\mu^+\mu^-} < 587.86$
ω region	$742.65 < m_{\mu^+\mu^-} < 822.65$
ρ region	$587.86 < m_{\mu^+\mu^-} < 742.66$ or $822.66 < m_{\mu^+\mu^-} < 965.20$
ϕ region	$979.46 < m_{\mu^+\mu^-} < 1059.46$

Normalisation to ϕ region



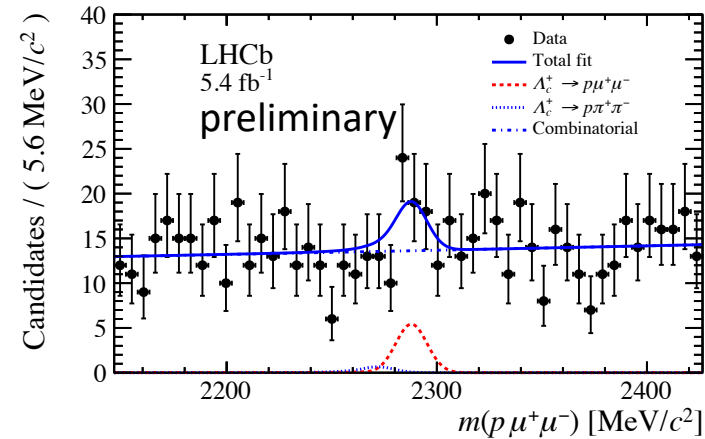
Fit results for the rare mode

Region	$\Lambda_c^+ \rightarrow p\mu^+\mu^-$ yield	$\Lambda_c^+ \rightarrow p\pi^+\pi^-$ yield	Combinatorial yield	Significance
<i>signal</i>	18.4 ± 9.7	2.7 ± 7.0	681.2 ± 27.9	2.0σ
<i>low-m</i>	1.4 ± 5.0	4.4 ± 3.8	240.7 ± 16.5	0.3σ
<i>high-m</i>	20.7 ± 8.4	3.8 ± 3.8	431.9 ± 22.1	2.8σ

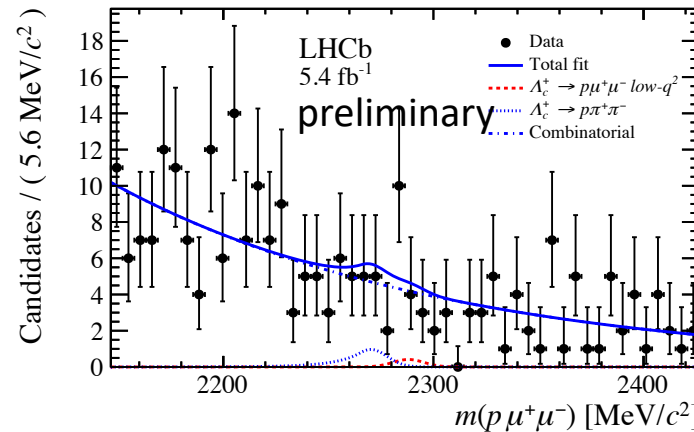
- In each region there are 4 parameters in the fit:

- signal yield
- combinatorial background yield
- combinatorial background slope
- yield of misID background yield (constrained from fit to data)

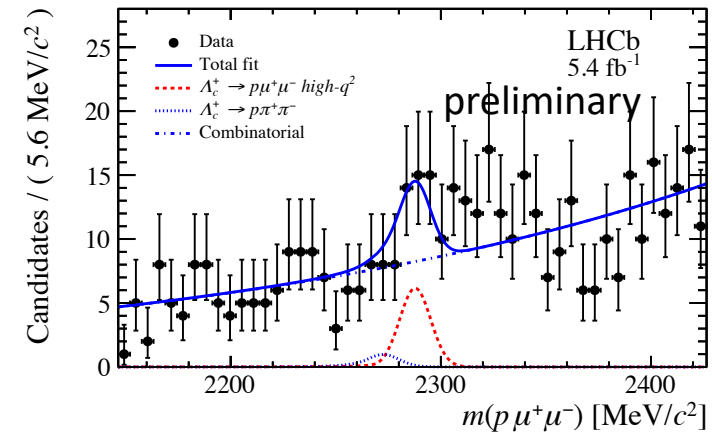
combined signal region



low-m

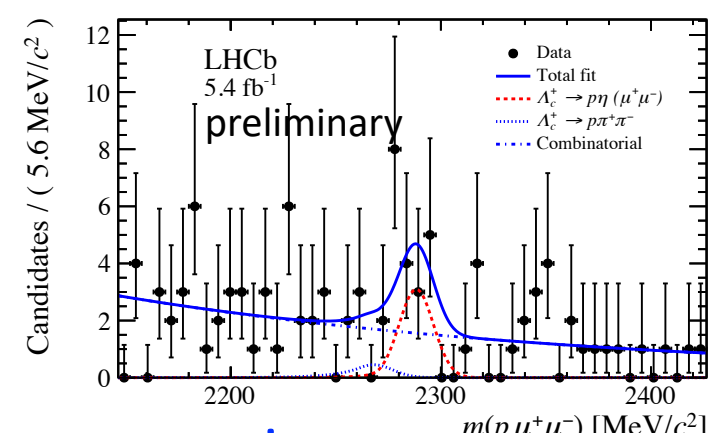
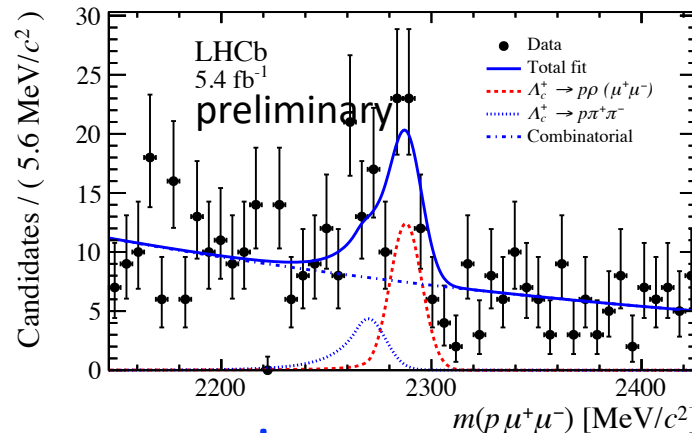
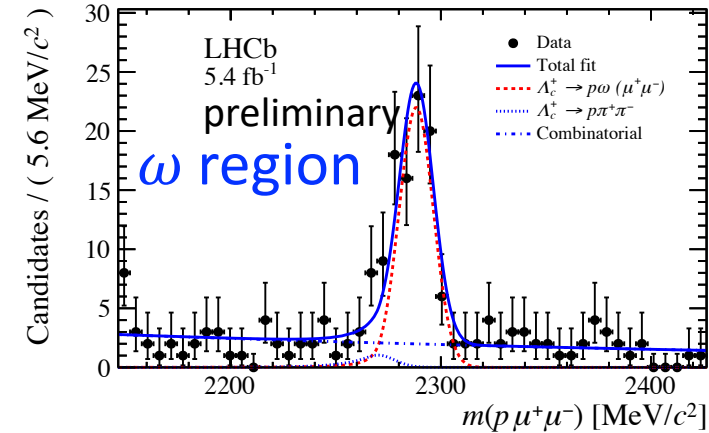
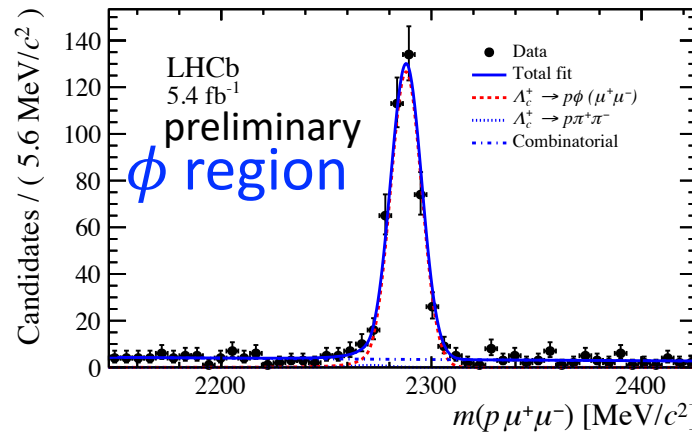


high-m



Fit results for the resonant modes

Region	$\Lambda_c^+ \rightarrow p\mu^+\mu^-$ yield	$\Lambda_c^+ \rightarrow p\pi^+\pi^-$ yield	Combinatorial yield	Significance
η	11.5 ± 4.8	2.2 ± 1.6	83.5 ± 9.8	3.0σ
ρ	43.2 ± 9.7	20.4 ± 6.3	381.8 ± 21.6	5.6σ
ω	80.9 ± 10.2	4.8 ± 2.1	101.0 ± 11.2	$> 7\sigma$
ϕ	423.0 ± 21.5	3.8 ± 2.4	173.2 ± 14.5	$> 7\sigma$



- the most abundant $\Lambda_c^+ \rightarrow p\phi(\rightarrow \mu^+\mu^-)$ channel is used for normalisation
- strong indication of a signal in previously unobserved $\Lambda_c^+ \rightarrow p\rho$ decay mode

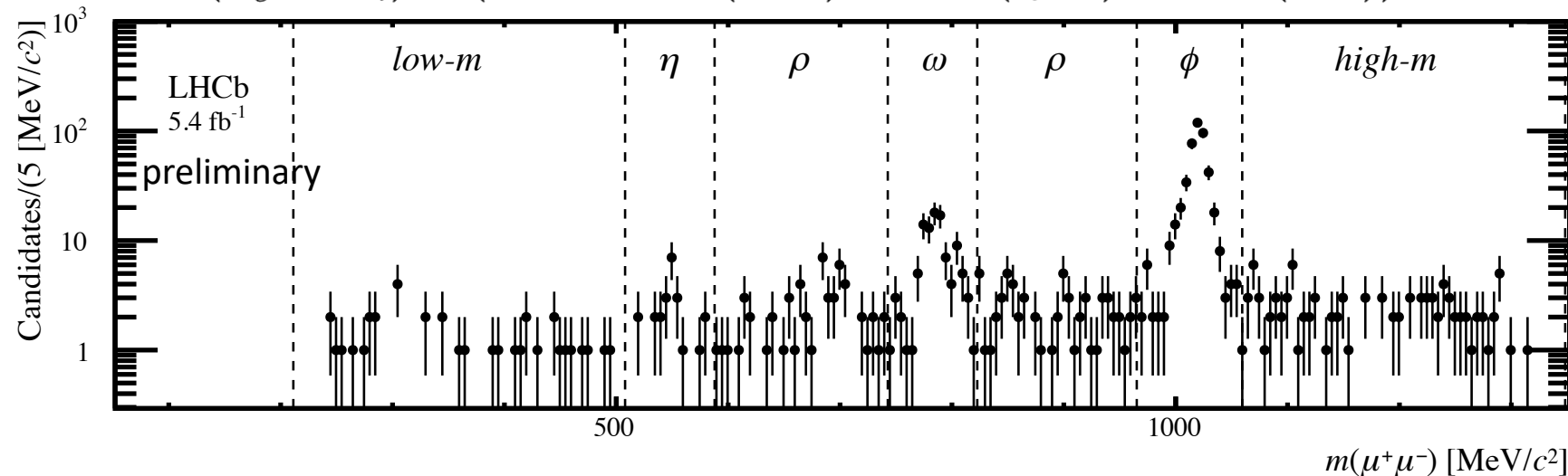
Summary

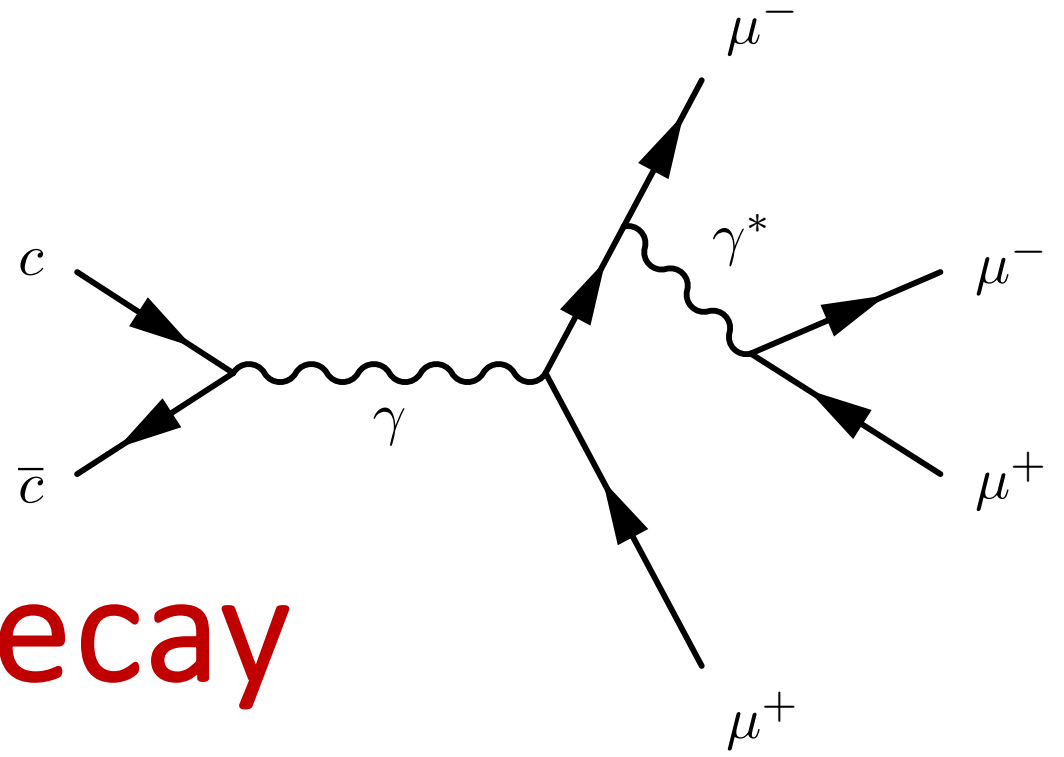
- Rare mode, extrapolating to full mass region from low- and high masses:
 - signal region (extrapolated): $\mathcal{B}(\Lambda_c^+ \rightarrow p\mu^+\mu^-) < 7.3 (8.2) \times 10^{-8}$ at 90% (95%) CL.
 - **low-mass:** $\mathcal{B}(\Lambda_c^+ \rightarrow p\mu^+\mu^-) < 6.5 (7.8) \times 10^{-8}$ at 90% (95%) CL
 - **high-mass:** $\mathcal{B}(\Lambda_c^+ \rightarrow p\mu^+\mu^-) < 11.8 (13.1) \times 10^{-8}$ at 90% (95%) CL
- Resonant mode mass regions (assuming no interference):

$$\mathcal{B}(\Lambda_c^+ \rightarrow p\omega) = (9.82 \pm 1.23 \text{ (stat.)} \pm 0.72 \text{ (syst.)} \pm 2.79 \text{ (ext.)}) \times 10^{-4}$$

$$\mathcal{B}(\Lambda_c^+ \rightarrow p\rho) = (1.52 \pm 0.34 \text{ (stat.)} \pm 0.14 \text{ (syst.)} \pm 0.24 \text{ (ext.)}) \times 10^{-3}$$

$$\mathcal{B}(\Lambda_c^+ \rightarrow p\eta) = (1.67 \pm 0.69 \text{ (stat.)} \pm 0.23 \text{ (syst.)} \pm 0.34 \text{ (ext.)}) \times 10^{-3}$$





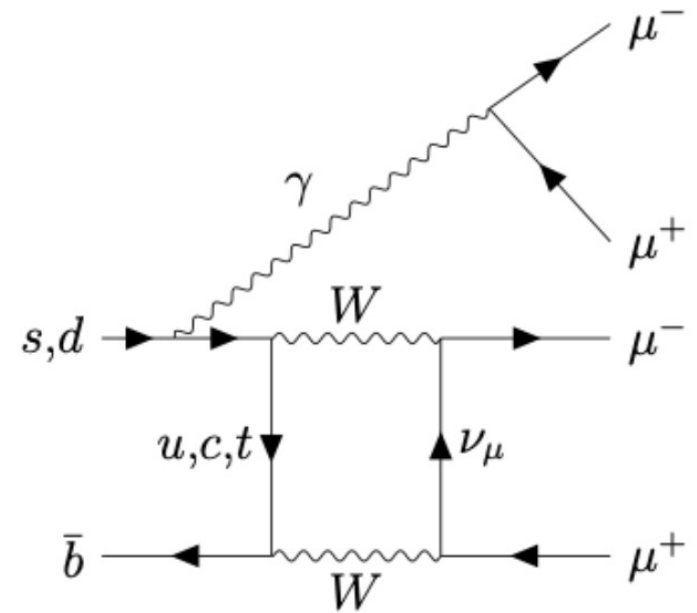
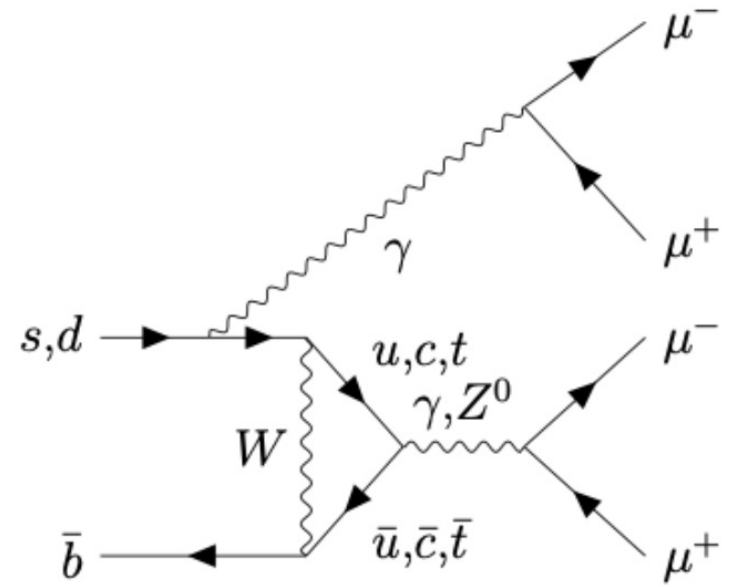
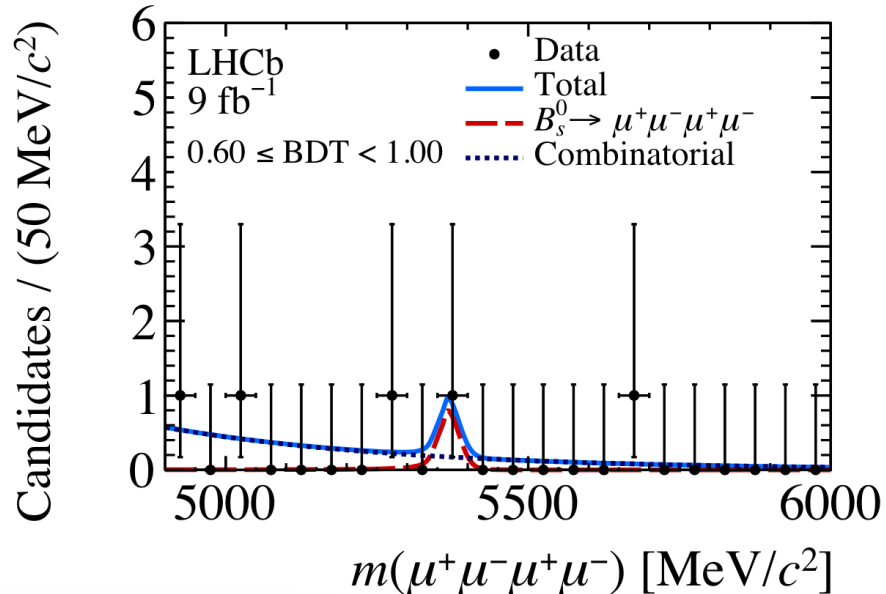
Study of the rare decay

$$J/\psi \rightarrow \mu^+ \mu^- \mu^+ \mu^-$$

[LHCb-CONF-2024-001](#)

B to 4 leptons?

- very rare process: penguin or box diagrams + initial (ISR)/final-state radiation (FSR)
- sensitive to the decays via intermediate narrow resonances
- predicted SM BFs ([Phys.Atom.Nucl. 81 \(2018\) 3, 347](#))
 - $O(10^{-10})$ for B_s
 - $O(10^{-12})$ for B^0
- best limits come from LHCb:
 - $< 8.6 \times 10^{-10}$ for B_s
 - $< 1.8 \times 10^{-10}$ for B^0



Observable 4-lepton decay: $J/\psi \rightarrow 4\mu$

- FSR of a virtual photon from the lepton

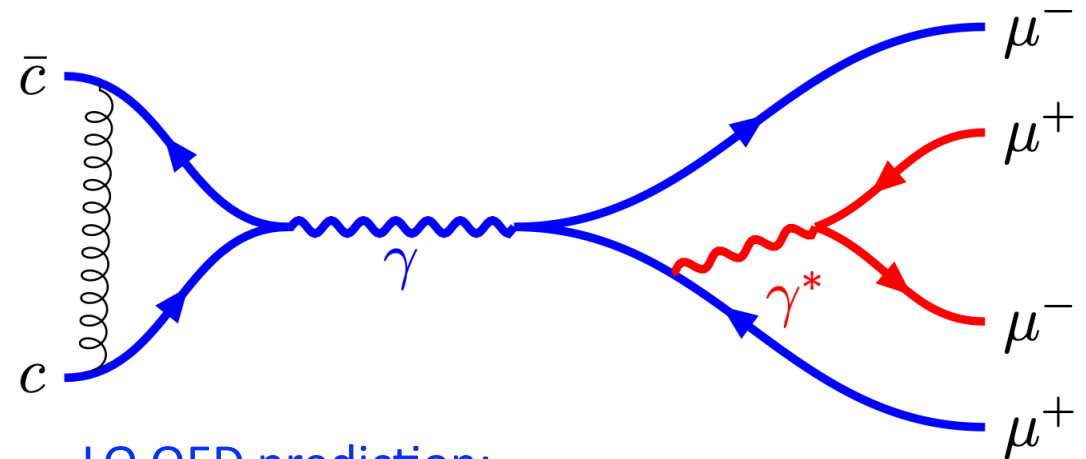
- ISR suppressed by C-parity:

- $J/\psi \rightarrow \gamma\gamma$ forbidden

- no significant contributions from intermediate vector resonances:

- $J/\psi \rightarrow VV \rightarrow 4\mu$ violates C parity

- a clean FSR process with future applications and sensitivity to possible BSM scenarios



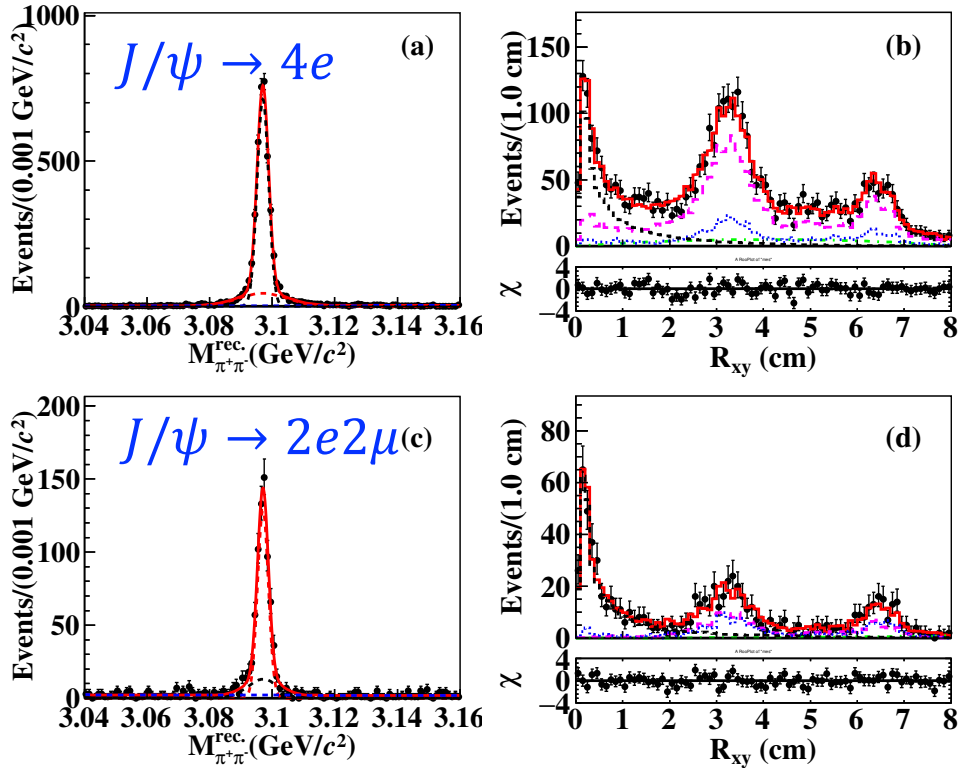
LO QED prediction:

$$\mathcal{B}(J/\psi \rightarrow 4\mu) = (9.74 \pm 0.05) \times 10^{-7}$$

Existing measurements

BES III experiment

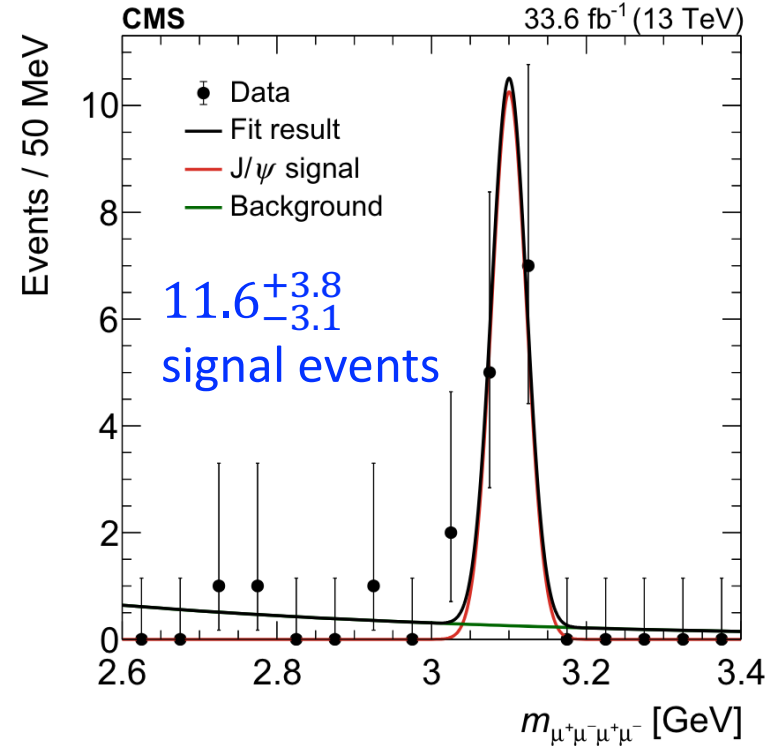
[Phys.Rev.D 109 \(2024\) 052006](#)



- $\mathcal{B}(J/\psi \rightarrow 4e) = (5.48 \pm 0.31 \pm 0.45) \times 10^{-5}$
- $\mathcal{B}(J/\psi \rightarrow 2e2\mu) = (3.53 \pm 0.22 \pm 0.13) \times 10^{-5}$
- $\mathcal{B}(J/\psi \rightarrow 4\mu) < 1.6 \times 10^{-6}$ @ 90% CL

CMS experiment

[arXiv:2403.11352](#)

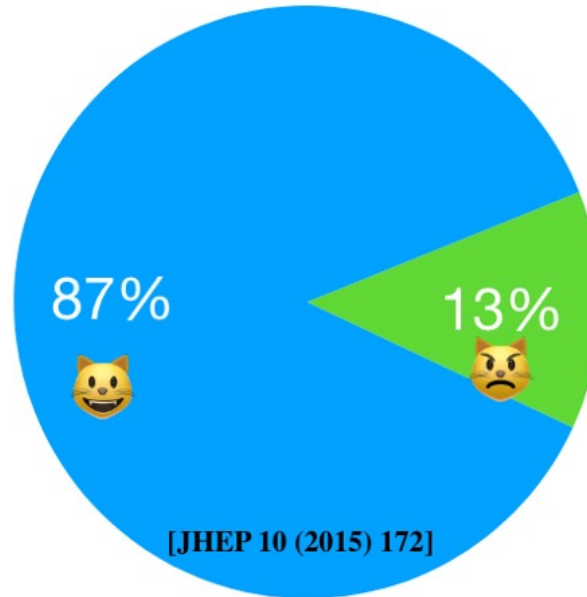
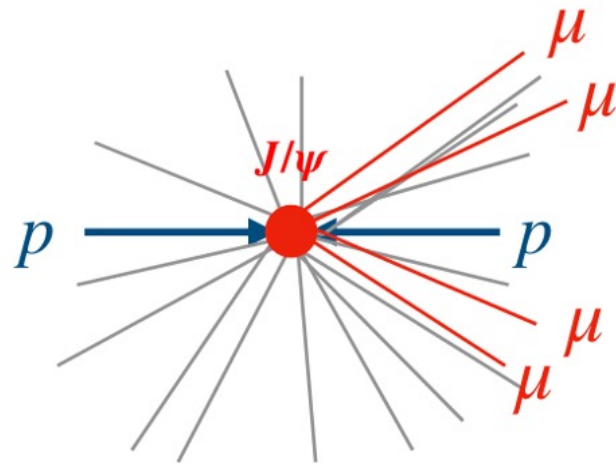


$$\mathcal{B}(J/\psi \rightarrow 4\mu) = (10.1^{+3.3}_{-2.7} \pm 0.4) \times 10^{-7}$$

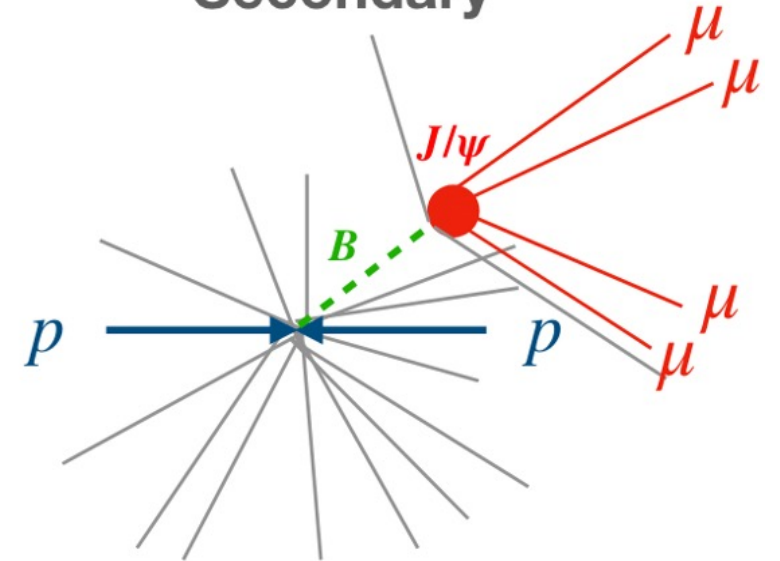
Analysis strategy

- measure $\mathcal{B}(J/\psi \rightarrow 4\mu)$ relative to normalisation channel $J/\psi \rightarrow 2\mu$
- use J/ψ from two origins:

Prompt



Secondary



- high production rate
- high background rates
- requires tight selection

- lower production rate
- lower background rates
- profit from B decay triggers

Results

- $J/\psi \rightarrow 4\mu$ observed in both samples with large significance ($\gg 5\sigma$)

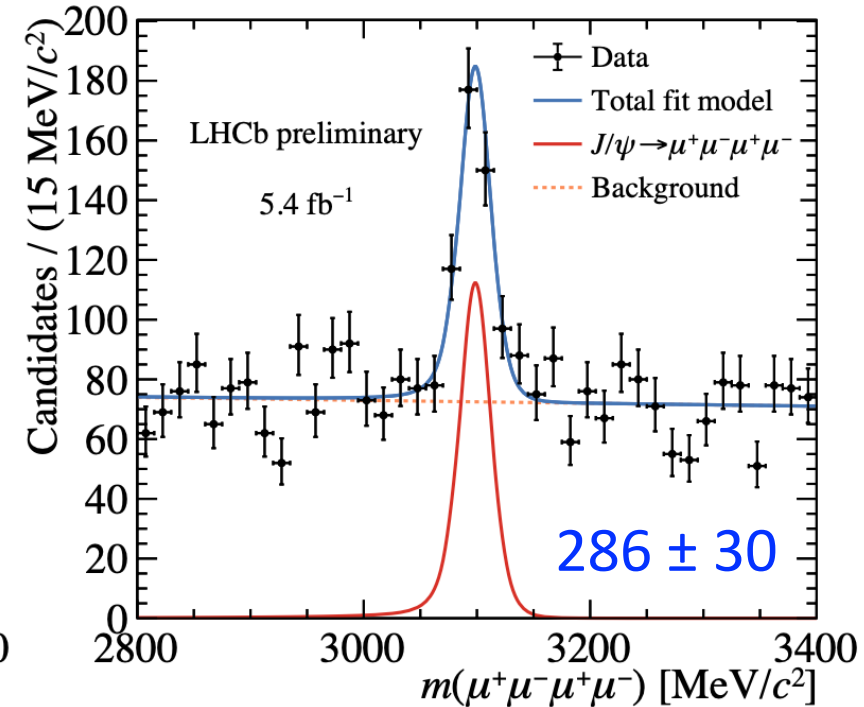
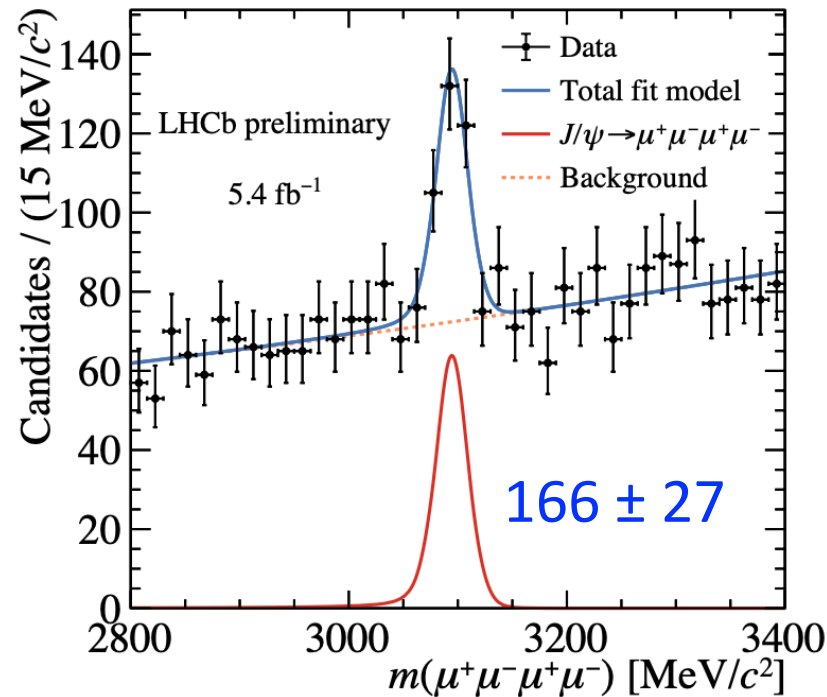
Prompt

Secondary

$$R_{BR} = (1.89 \pm 0.17 \pm 0.09) \times 10^{-5}$$

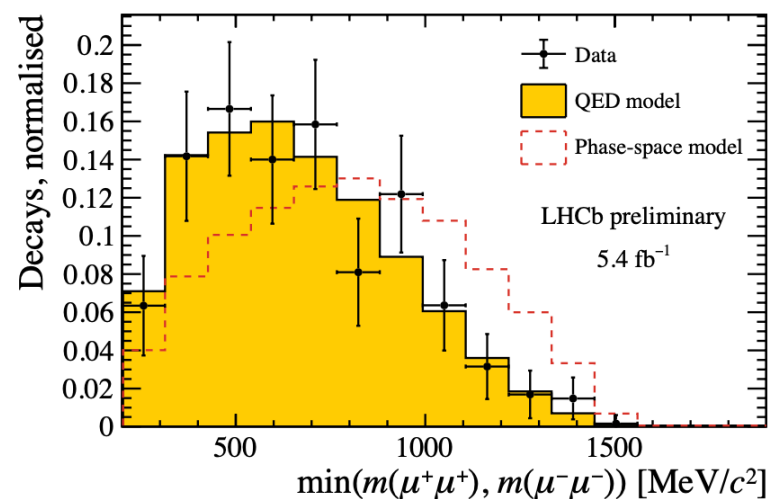
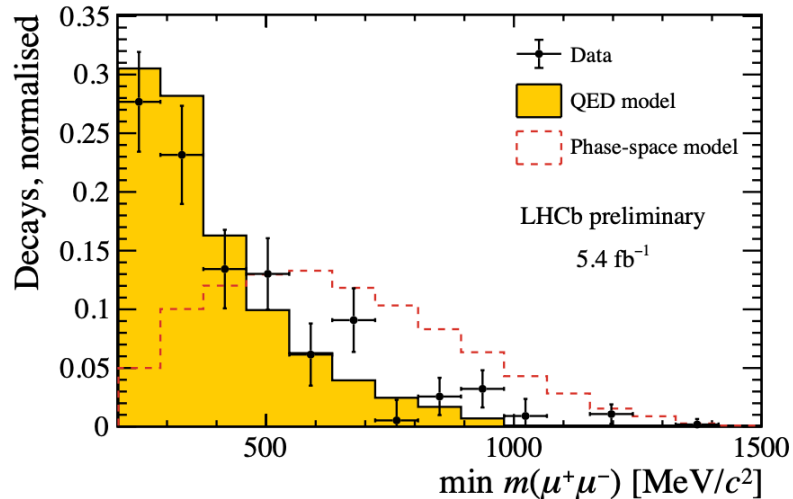
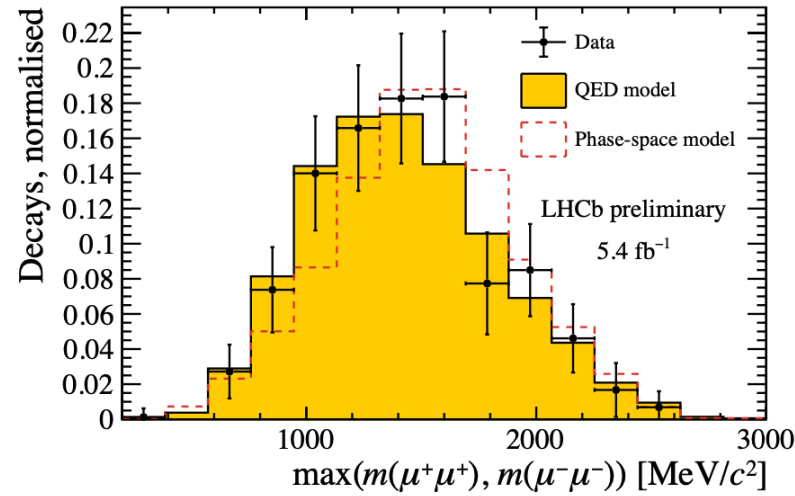
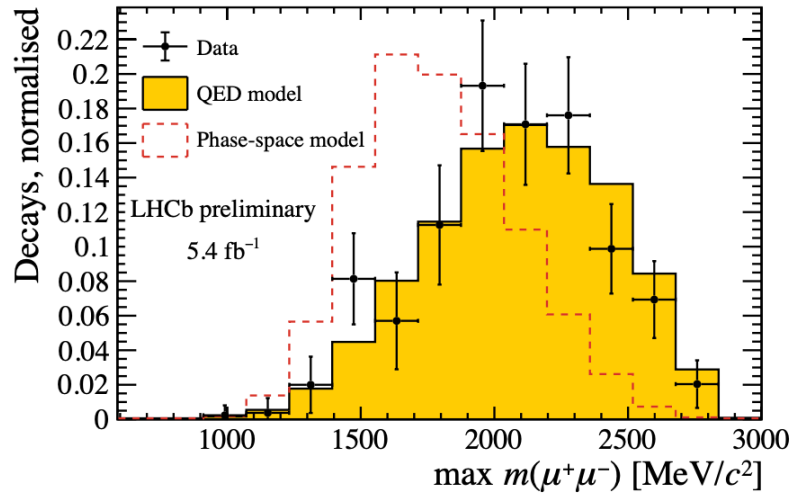
$$\mathcal{B}(J/\psi \rightarrow \mu^+\mu^-\mu^+\mu^-) = (11.3 \pm 1.0 \pm 0.5 \pm 0.1) \times 10^{-7}$$

- most precise measurement to date
- consistent with the SM prediction at the level of 1.4σ



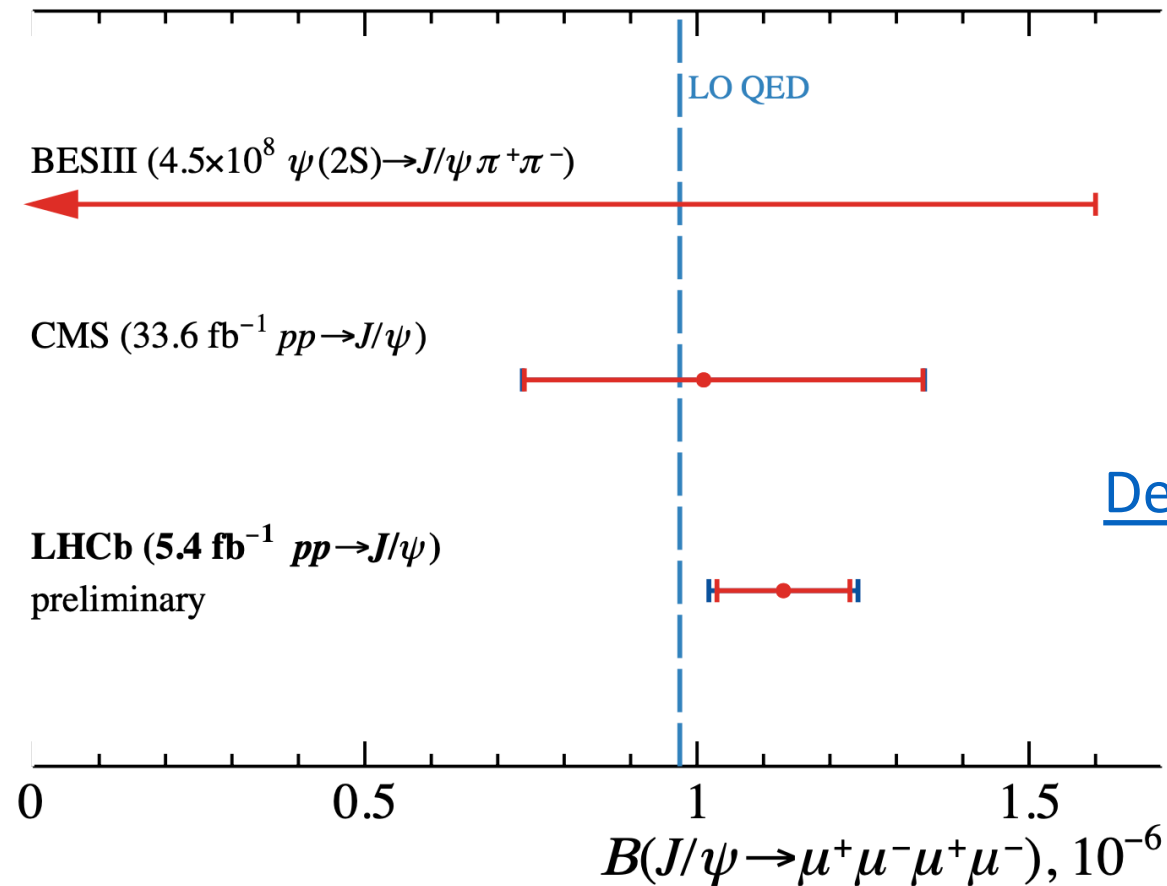
Kinematic distributions

Secondary



- size of the sample allows to study kinematic distributions
- found to be consistent with the LO QED model
- *many thanks to BES III colleagues for providing the code for the model!*
- PHSP model significantly differs

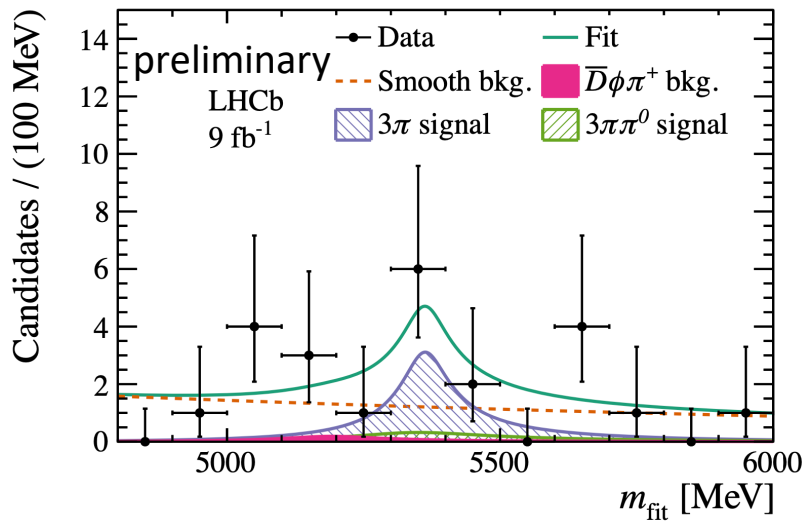
Existing $J/\psi \rightarrow 4\mu$ measurements summary



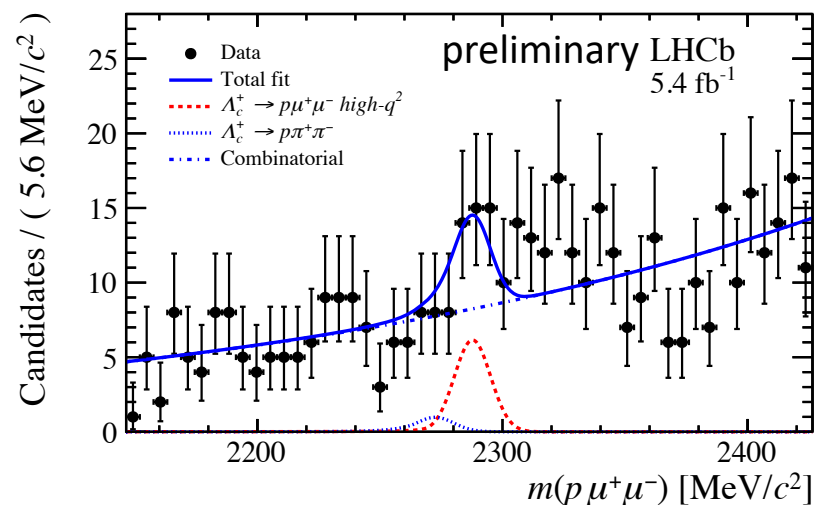
[Dedicated LHCb public page](#)

From unseen to observed to detailed study!

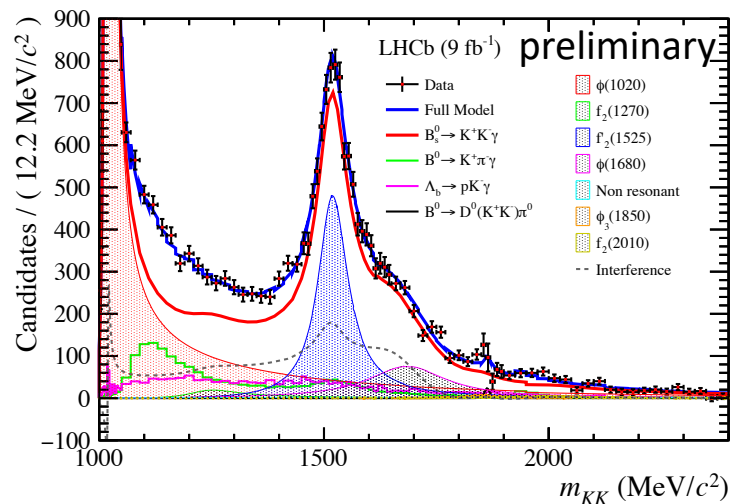
No LFV yet



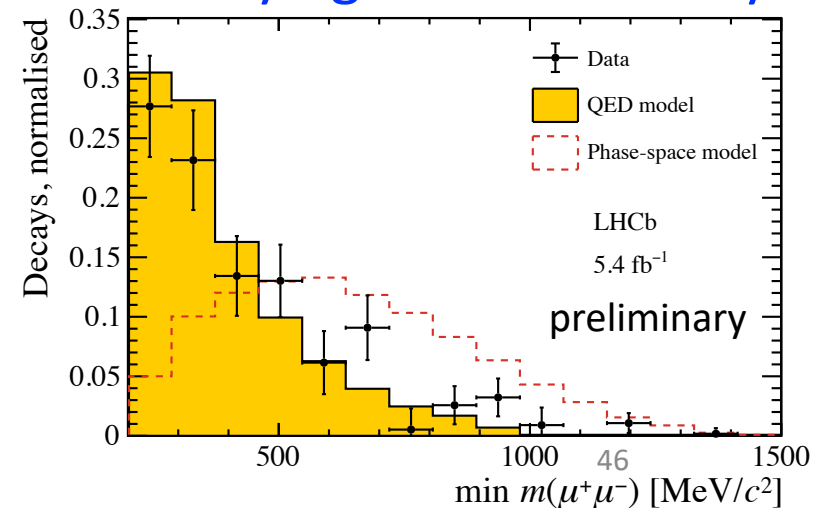
Closing in to charm FCNC



Observing a new radiative B_s^0 decay



Studying a rare 4ℓ decay



Outlook

LHCb DETECTOR LS2 UPGRADES

VELO: NEW SILICON PIXEL DETECTOR

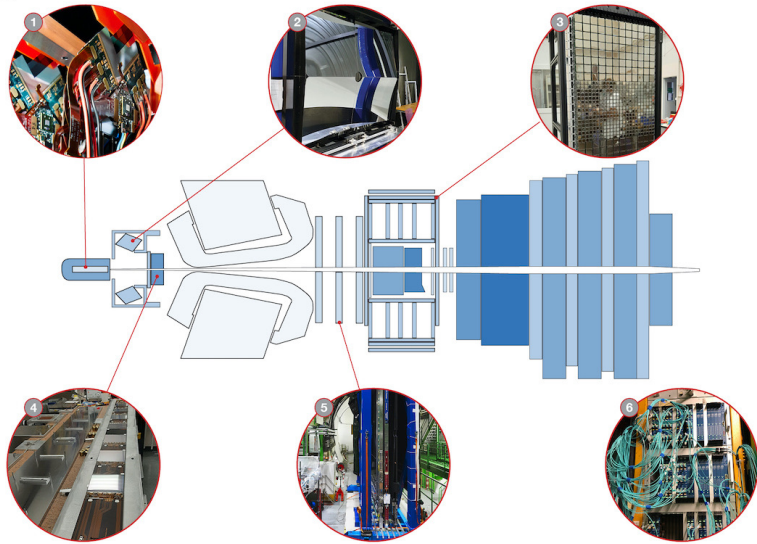
Vertex Locator (VELO) replaced by a new silicon pixel detector, installed as close as 5.1 mm to the proton beams.

RICH1

New optics of RICH1 mirrors, with larger curvature radius.

RICH2

New multi-anode photomultipliers replaced the hybrid photon detectors (HPD) in RICH1 and RICH2.



TRACKER: New UT

New high granularity silicon microstrip upstream tracker (UT).

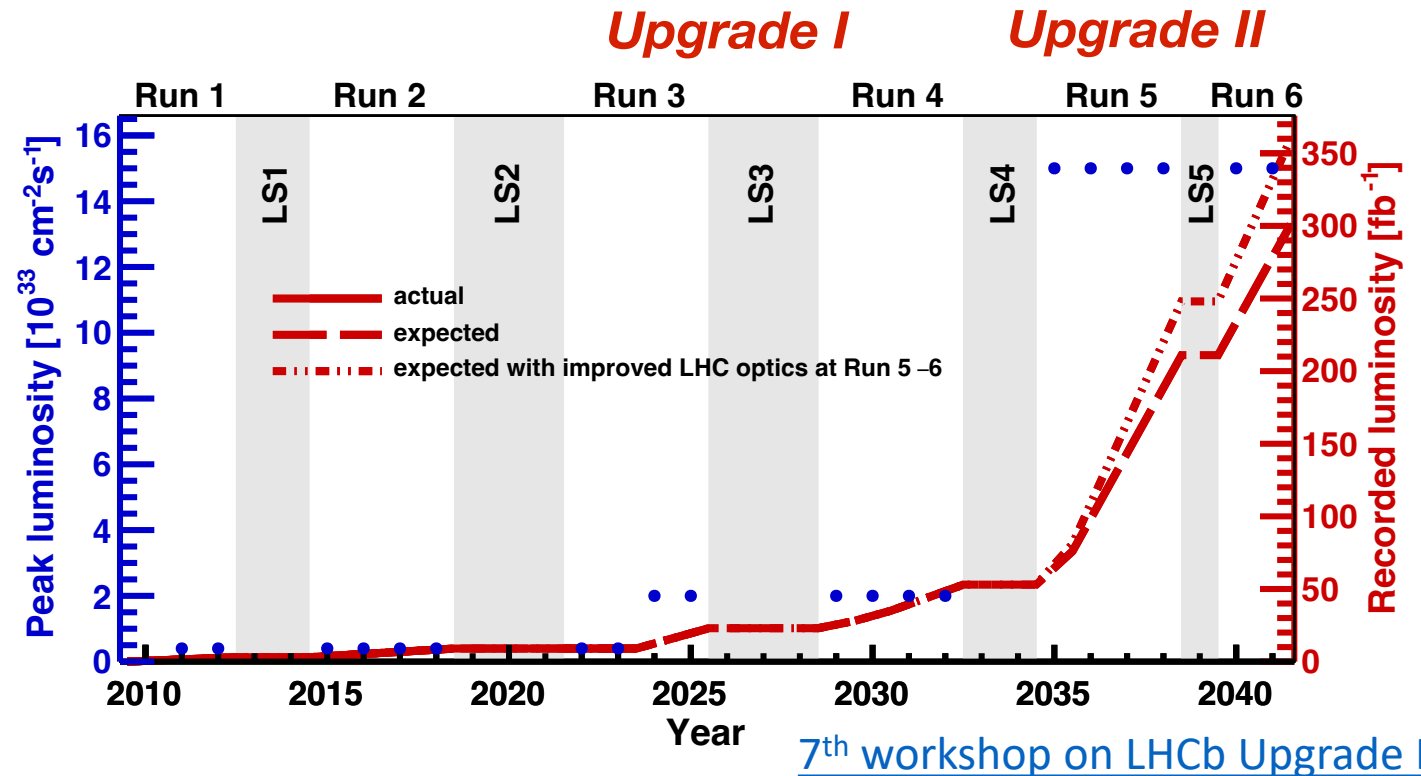
TRACKER: SCI-FI

Three new scintillating fibre tracker (Sci-Fi) stations.

FRONT-END ELECTRONICS

All front-end electronics (i.e. those connected directly to the detectors) have been modified.

LHCb Upgrade



- Unique LHCb coverage and capabilities leads to precision studies not available elsewhere
- Developments with the upgraded detector will allow to significantly expand the **rare** programme!

Extra slides

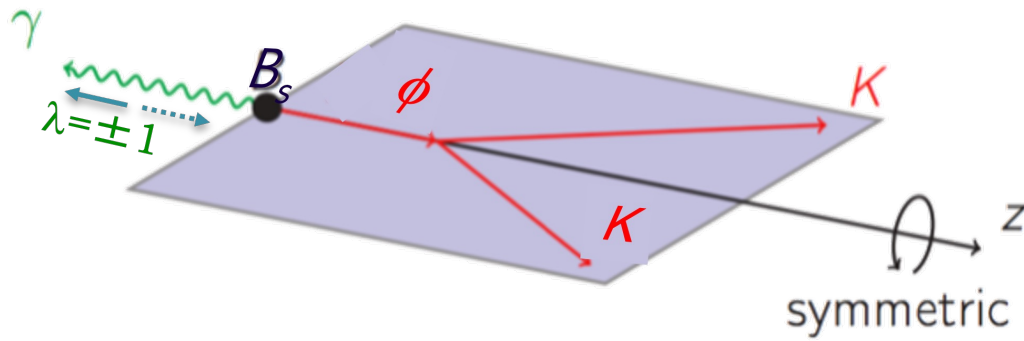
$B_S^0 \rightarrow K^+ K^- \gamma$: helicity angle

- $\cos\theta_{KK} = \frac{(s_{K^+\gamma} - s_{K^-\gamma})m_{KK}}{4M_{B_S}q_Rq_{B_S}}$, where

- $s_{ij} = m_{ij}^2$

- q_R - kaon momentum in the dikaon restframe

- q_{B_S} - dikaon momentum in the B_S^0 restframe



Amplitude model: (m_{KK}, θ_{KK}) PDF

- Global PDF: $\mathcal{P}(m_{KK}, \theta_{KK}) = \underbrace{\mathcal{N}_s \mathcal{P}_s}_{\text{signal}} + \underbrace{\sum_{bkg} \mathcal{N}_{bkg} \mathcal{P}_{bkg}}_{\text{peaking backgrounds}}$

- Signal PDF:

- $\mathcal{P}(m_{KK}, \theta_{KK}) = \varepsilon(m_{KK}, |\cos\theta_{KK}|) \cdot \mathcal{J}_3(m_{KK}) \sum_{P=+,-} \left| \sum_{R_P} C_{R_P} \cdot \mathcal{A}_{R_P}(m_{KK}, |\cos\theta_{KK}|) \right|^2$
- $\varepsilon(m_{KK}, |\cos\theta_{KK}|)$ - 2D acceptance
- $\mathcal{J}_3(m_{KK})$ – the three-body phase space Jacobian
- C_{R_P} - complex coefficients
- $\mathcal{A}_R(m_{KK}, |\cos\theta_{KK}|) = BW_R(m_{KK}) \cdot d_{10}^{JR}(\theta_{KK})$ - amplitudes
- $d_{10}^{JR}(\theta_{KK})$ - Wigner d-functions, representing the matrix elements of the operator rotating the angular momentum basis from the B decay axis to the dikaon decay axis
- m_{KK} resolutions included in the relativistic BW using analytical convolution
[\[J.Math.Anal.Appl. 463 \(2018\) 2, 1040\]](#)

Amplitude fit: minimization procedure

sWeighted unbinned extended log-likelihood fit $-\ln \mathcal{L}_\omega(\vec{p}) = -\sum_i^N \omega_i \ln \mathcal{P}(\vec{o}_i; \vec{p})$

Fit parameters $\vec{p} =$:: N isobars and (N-1) phases	$c_R e^{i\delta_R}$, relative to $c_{1020}=1$ and $\delta_{1020}=\delta_{1525}=0$
	:: 5 lineshape parameters	μ and Γ for ϕ_{1020} and $f'_{2(1525)} + \phi_{1020}$ radius
	:: 4 yields	N_s signal and N_{B^0} , N_{Λ_b} , N_{D^0} backgrounds

Other lineshape parameters are fixed to world-average values.

Meson radius **free to vary for ϕ_{1020}**

fixed to 3.0 c/GeV for heavy resonances.

Mass resolutions fixed to MC simulation values

fit-fractions:

$$\mathcal{F}_R = |c_R|^2 \frac{\int_0^{+1} \int_{2m_K}^{2.4\text{GeV}c^{-2}} |\mathcal{A}_R(m_{KK}, |\cos\theta_{KK}|)|^2 d\phi_3}{\int_0^{+1} \int_{2m_K}^{2.4\text{GeV}c^{-2}} \sum_P |\sum_{R_P} c_{R_P} \cdot \mathcal{A}_{R_P}(m_{KK}, |\cos\theta_{KK}|)|^2 d\phi_3}$$

$B_S^0 \rightarrow K^+ K^- \gamma$: systematic uncertainties

		$m_{KK\gamma}$ fit	Acceptance	Amp. fit	Isobar model	Total
$\phi(1020)$	\mathcal{F}_R (%)	$\begin{matrix} +0.2 \\ -0.7 \end{matrix}$	$\begin{matrix} +0.9 \\ -0.4 \end{matrix}$	$\begin{matrix} +0.3 \\ -0.9 \end{matrix}$	$\begin{matrix} +0.3 \\ -0.5 \end{matrix}$	$\begin{matrix} +1.0 \\ -1.2 \end{matrix}$
	μ_R (keV/c ²)	$\begin{matrix} +5 \\ -6 \end{matrix}$	$\begin{matrix} +5 \\ -6 \end{matrix}$	$\begin{matrix} +5 \\ -4 \end{matrix}$	$\begin{matrix} +6 \\ -14 \end{matrix}$	$\begin{matrix} +11 \\ -16 \end{matrix}$
	Γ_R (keV/c ²)	$\begin{matrix} +3 \\ -10 \end{matrix}$	$\begin{matrix} +8 \\ -7 \end{matrix}$	$\begin{matrix} +14 \\ -62 \end{matrix}$	$\begin{matrix} +20 \\ -82 \end{matrix}$	$\begin{matrix} +26 \\ -103 \end{matrix}$
	r_ϕ ((GeV/c) ⁻¹)	$\begin{matrix} +0.02 \\ -0.07 \end{matrix}$	$\begin{matrix} +0.05 \\ -0.04 \end{matrix}$	$\begin{matrix} +0.05 \\ -0.06 \end{matrix}$	± 0.09	± 0.12
$f_2(1270)$	\mathcal{F}_R (%)	$\begin{matrix} +0.09 \\ -0.22 \end{matrix}$	$\begin{matrix} +0.04 \\ -0.07 \end{matrix}$	$\begin{matrix} +0.13 \\ -0.21 \end{matrix}$	$\begin{matrix} +0.09 \\ -0.13 \end{matrix}$	$\begin{matrix} +0.2 \\ -0.3 \end{matrix}$
	$\mathcal{F}_R/\mathcal{F}_\phi$ (%)	$\begin{matrix} +0.13 \\ -0.31 \end{matrix}$	$\begin{matrix} +0.05 \\ -0.10 \end{matrix}$	$\begin{matrix} +0.2 \\ -0.3 \end{matrix}$	$\begin{matrix} +0.13 \\ -0.19 \end{matrix}$	$\begin{matrix} +0.3 \\ -0.5 \end{matrix}$
	δ_R (deg.)	$\begin{matrix} +6.3 \\ -3.8 \end{matrix}$	$\begin{matrix} +1.1 \\ -0.9 \end{matrix}$	$\begin{matrix} +5.6 \\ -8.5 \end{matrix}$	$\begin{matrix} +23.1 \\ -14.1 \end{matrix}$	$\begin{matrix} +24.6 \\ -16.9 \end{matrix}$
$f_2'(1525)$	\mathcal{F}_R (%)	$\begin{matrix} +0.3 \\ -0.2 \end{matrix}$	$\begin{matrix} +0.2 \\ -0.1 \end{matrix}$	$\begin{matrix} +0.6 \\ -0.3 \end{matrix}$	$\begin{matrix} +0.6 \\ -0.2 \end{matrix}$	$\begin{matrix} +0.9 \\ -0.4 \end{matrix}$
	$\mathcal{F}_R/\mathcal{F}_\phi$ (%)	$\begin{matrix} +0.3 \\ -0.1 \end{matrix}$	$\begin{matrix} +0.3 \\ -0.4 \end{matrix}$	$\begin{matrix} +0.9 \\ -0.2 \end{matrix}$	$\begin{matrix} +0.9 \\ -0.2 \end{matrix}$	$\begin{matrix} +1.3 \\ -0.5 \end{matrix}$
	μ_R (MeV/c ²)	$\begin{matrix} +0.3 \\ -0.8 \end{matrix}$	± 0.2	$\begin{matrix} +0.6 \\ -0.5 \end{matrix}$	$\begin{matrix} +1.2 \\ -1.7 \end{matrix}$	$\begin{matrix} +1.4 \\ -1.9 \end{matrix}$
	Γ_R (MeV/c ²)	$\begin{matrix} +0.6 \\ -0.9 \end{matrix}$	$\begin{matrix} +0.8 \\ -0.4 \end{matrix}$	$\begin{matrix} +2.0 \\ -0.6 \end{matrix}$	$\begin{matrix} +2.5 \\ -1.0 \end{matrix}$	$\begin{matrix} +3.4 \\ -1.5 \end{matrix}$
$\phi(1680)$	\mathcal{F}_R (%)	$\begin{matrix} +0.3 \\ -0.5 \end{matrix}$	± 0.2	± 0.3	± 0.5	± 0.7
	$\mathcal{F}_R/\mathcal{F}_\phi$ (%)	$\begin{matrix} +0.4 \\ -0.6 \end{matrix}$	$\begin{matrix} +0.3 \\ -0.3 \end{matrix}$	$\begin{matrix} +0.5 \\ -0.4 \end{matrix}$	± 0.7	$\begin{matrix} +1.0 \\ -1.1 \end{matrix}$
	δ_R (deg.)	$\begin{matrix} +2.7 \\ -3.1 \end{matrix}$	$\begin{matrix} +1.2 \\ -1.4 \end{matrix}$	$\begin{matrix} +3.9 \\ -1.7 \end{matrix}$	$\begin{matrix} +6.7 \\ -6.9 \end{matrix}$	$\begin{matrix} +8.3 \\ -7.9 \end{matrix}$
$\phi_3(1850)$	\mathcal{F}_R (%)	$\begin{matrix} +0.13 \\ -0.07 \end{matrix}$	± 0.03	$\begin{matrix} +0.07 \\ -0.04 \end{matrix}$	$\begin{matrix} +0.12 \\ -0.10 \end{matrix}$	$\begin{matrix} +0.19 \\ -0.13 \end{matrix}$
	$\mathcal{F}_R/\mathcal{F}_\phi$ (%)	$\begin{matrix} +0.19 \\ -0.10 \end{matrix}$	$\begin{matrix} +0.05 \\ -0.04 \end{matrix}$	$\begin{matrix} +0.10 \\ -0.06 \end{matrix}$	$\begin{matrix} +0.17 \\ -0.14 \end{matrix}$	$\begin{matrix} +0.3 \\ -0.2 \end{matrix}$
	δ_R (deg.)	$\begin{matrix} +1.4 \\ -4.7 \end{matrix}$	$\begin{matrix} +2.7 \\ -1.5 \end{matrix}$	$\begin{matrix} +4.1 \\ -3.2 \end{matrix}$	$\begin{matrix} +11.5 \\ -10.5 \end{matrix}$	$\begin{matrix} +12.6 \\ -12.1 \end{matrix}$
$f_2(2010)$	\mathcal{F}_R (%)	$\begin{matrix} +0.08 \\ -0.01 \end{matrix}$	$\begin{matrix} +0.02 \\ -0.07 \end{matrix}$	$\begin{matrix} +0.14 \\ -0.07 \end{matrix}$	$\begin{matrix} +0.11 \\ -0.10 \end{matrix}$	$\begin{matrix} +0.20 \\ -0.14 \end{matrix}$
	$\mathcal{F}_R/\mathcal{F}_\phi$ (%)	$\begin{matrix} +0.11 \\ -0.01 \end{matrix}$	$\begin{matrix} +0.02 \\ -0.10 \end{matrix}$	$\begin{matrix} +0.21 \\ -0.10 \end{matrix}$	$\begin{matrix} +0.16 \\ -0.14 \end{matrix}$	$\begin{matrix} +0.3 \\ -0.2 \end{matrix}$
	δ_R (deg.)	$\begin{matrix} +17.1 \\ -15.9 \end{matrix}$	$\begin{matrix} +9.1 \\ -2.8 \end{matrix}$	$\begin{matrix} +20.5 \\ -11.7 \end{matrix}$	$\begin{matrix} +43.7 \\ -55.1 \end{matrix}$	$\begin{matrix} +52.1 \\ -58.6 \end{matrix}$
(KK) _{NR}	\mathcal{F}_R (%)	$\begin{matrix} +0.21 \\ -0.08 \end{matrix}$	$\begin{matrix} +0.04 \\ -0.14 \end{matrix}$	$\begin{matrix} +0.23 \\ -0.12 \end{matrix}$	$\begin{matrix} +0.12 \\ -0.09 \end{matrix}$	$\begin{matrix} +0.3 \\ -0.2 \end{matrix}$
	$\mathcal{F}_R/\mathcal{F}_\phi$ (%)	$\begin{matrix} +0.31 \\ -0.11 \end{matrix}$	$\begin{matrix} +0.07 \\ -0.21 \end{matrix}$	$\begin{matrix} +0.34 \\ -0.17 \end{matrix}$	$\begin{matrix} +0.17 \\ -0.12 \end{matrix}$	$\begin{matrix} +0.5 \\ -0.3 \end{matrix}$
	δ_R (deg.)	$\begin{matrix} +1.9 \\ -4.5 \end{matrix}$	$\begin{matrix} +1.7 \\ -2.8 \end{matrix}$	$\begin{matrix} +6.1 \\ -6.7 \end{matrix}$	$\begin{matrix} +5.5 \\ -3.9 \end{matrix}$	$\begin{matrix} +8.5 \\ -9.4 \end{matrix}$

- Mass fit and sWeights extraction:
 - vary signal and bkg models
 - extract sWeights in separate m_{KK} bins
- 2D acceptance:
 - vary acceptance model
 - vary with MC simulation stat. unc.
 - simulation weighting
- Amplitude fit:
 - PDF definitions: allow for B_S^0 asymmetry
 - vary binning scheme for peaking bkg,
 - test neglected bkg
- Isobar model:
 - use alternative resonant structure
 - vary fixed mass & width, meson radius

$B_s^0 \rightarrow \phi \mu^\pm \tau^\mp$: systematic uncertainties

Source	$\delta\alpha_{3\pi} \times 10^{-5}$	$\delta\alpha_{3\pi\pi^0} \times 10^{-5}$
$\psi(2S)\phi$ branching fraction	1.18	0.26
Other branching fractions	0.18	0.05
Normalization yield	0.40	0.09
Size of simulated samples	0.47	0.15
τ decay model	0.61	0.13
Signal decay model	0.90	0.18
Other efficiency uncertainties	0.68	0.16
Total	1.9	0.4

$\Lambda_c^+ \rightarrow p\mu^+\mu^-$: systematic uncertainties

Uncertainty source	η [%]	ρ [%]	ω [%]
Normalisation channel	5.60	5.60	5.60
Efficiency ratio (stat.)	12.91	5.33	4.58
Efficiency ratio (syst.)	1.65	1.65	1.65
Shape of signal	0.60	1.66	1.16
Shape of $\Lambda_c^+ \rightarrow p\pi^+\pi^-$	0.39	5.27	1.23
Shape of combinatorial	0.08	0.03	0.01
$\Lambda_c^+ \rightarrow p\pi^+\pi^-$ decay model	0.08	0.08	0.08
Fit bias	0.33	0.12	0.07
Total	14.02	9.40	7.30

$J/\psi \rightarrow \mu^+ \mu^- \mu^+ \mu^-$: systematic uncertainties

Source	Secondary	Prompt	Correlated?
Size of simulated samples	0.6	0.8	no
Treatment of simulation	1.1	0.8	yes
Fraction of secondary J/ψ component	0.3	0.2	no
Kinematic calibration	0.5	0.2	no
Hardware trigger calibration	0.3	0.4	yes
Software trigger calibration	1.0	0.4	no
Tracking calibration	2.3	1.8	yes
Muon ID calibration	3.1	5.8	yes
Mass modelling	0.6	0.7	no
Multiple candidate selection	0.6	0.8	no
Total uncorrelated	1.5	1.5	–
Total correlated	4.1	6.2	–
Total systematic uncertainty	4.4	6.3	–
Statistical uncertainty	10.5	16.2	no